

Precision Measurements in Astronomy

$P = 5.757451924362137 \text{ ms}$

Ajit Kembhavi
IUCAA

Astronomical Data Over the Centuries

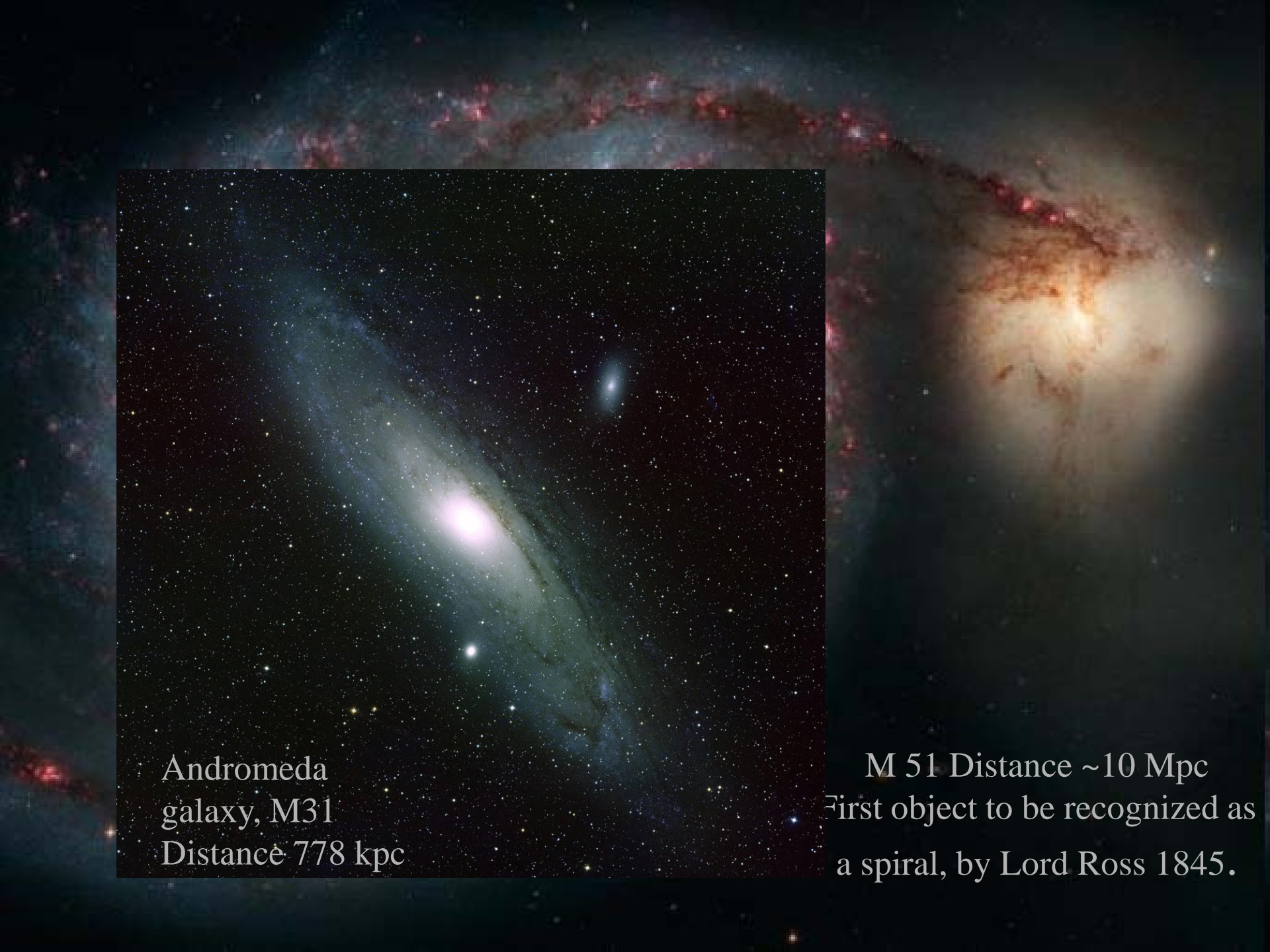
Hipparchus discovered the
precession of the equinoxes.

USNO-B1
1.05 billion

GSC II
0.9 billion



Hubble's Constant



Andromeda
galaxy, M31
Distance 778 kpc

M 51 Distance ~10 Mpc
First object to be recognized as
a spiral, by Lord Ross 1845.

Coma Cluster



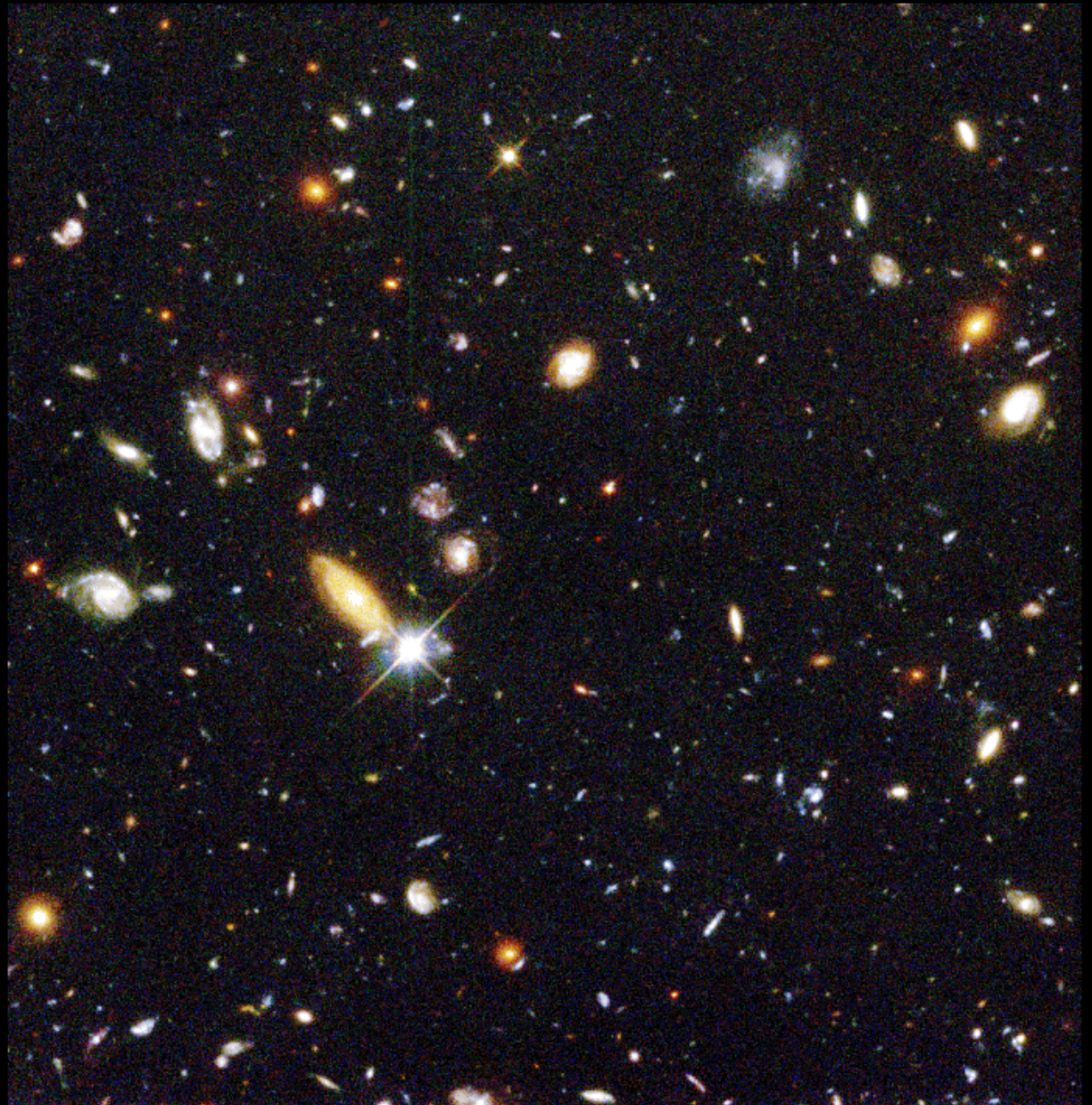
NGC
4889

NGC
4874

Rich cluster
containing ~1000
identified galaxies.
Distance 99 Mpc

Hubble Deep Field

Deep exposure of a region in Ursa major 7 sq arcmin in four filters. 30.3 hr at 606 nm. Most of the ~3000 objects in the field are galaxies.

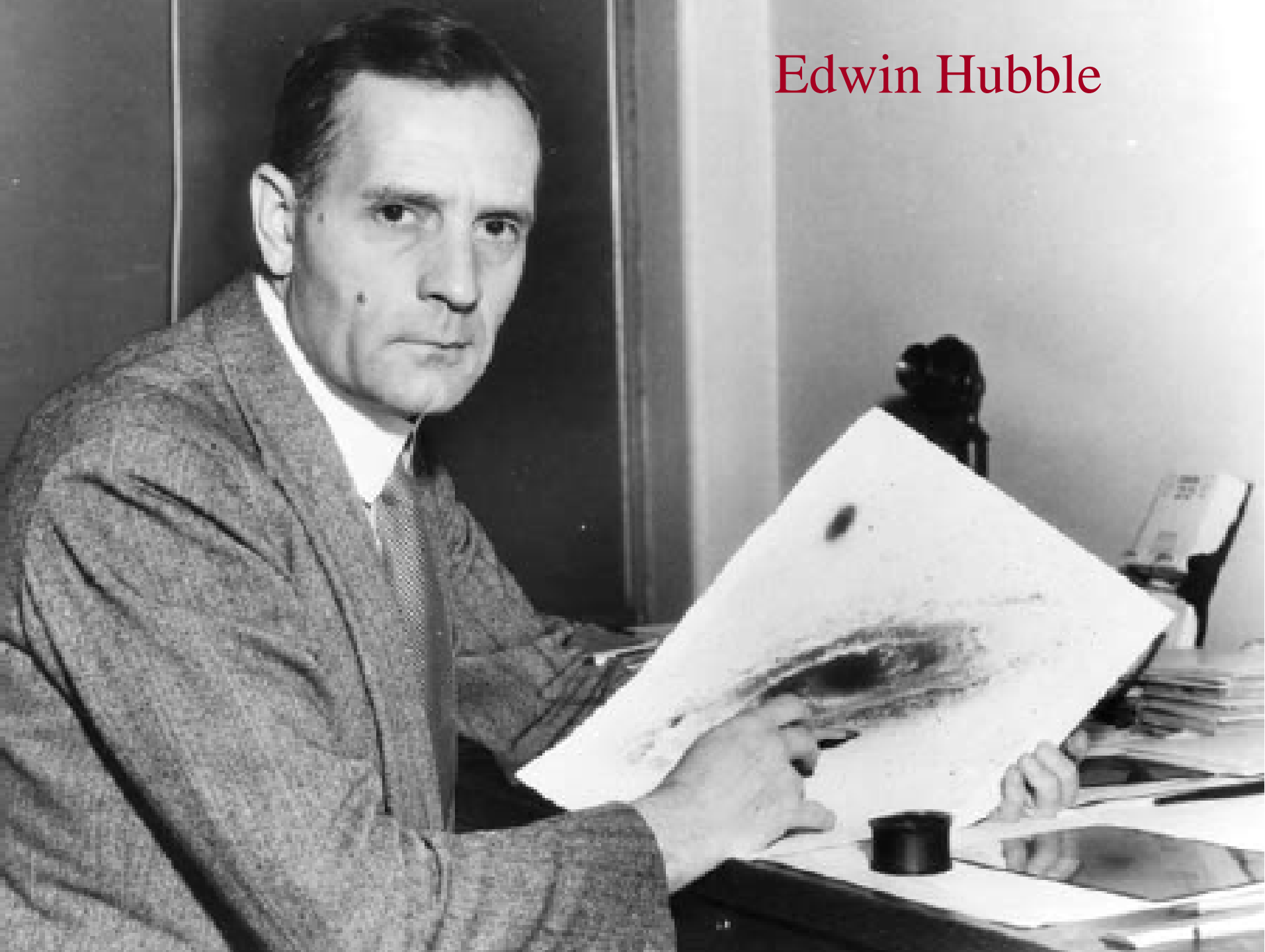


Hubble Deep Field

HST · WFPC2

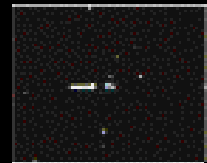
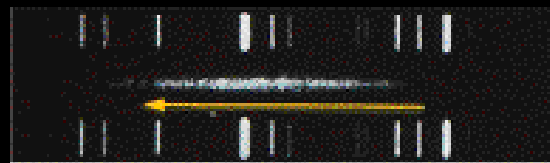
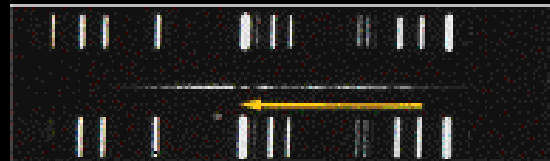
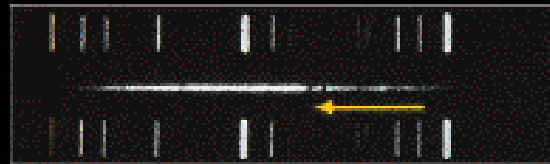
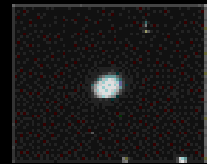
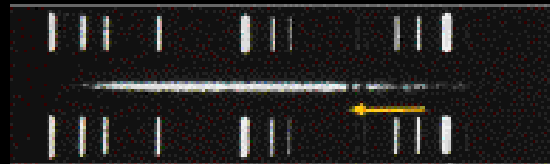
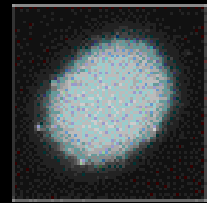
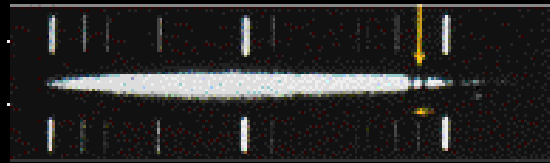
PRC96-01a · ST ScI OPO · January 15, 1996 · R. Williams (ST ScI), NASA

Edwin Hubble



Galaxy Redshift

First measured
by Vesto Slipher
1912



Redshift and the Doppler Effect

$$1 + z = \frac{\lambda_o}{\lambda_e} = \sqrt{\frac{c + v}{c - v}}$$

Doppler
Effect

$$z \simeq \frac{v}{c}, \quad v \ll c$$

$v = cz$

$$v = H_0 D$$

Hubble's
Law

$$D = \left(\frac{c}{H_0} \right) z$$

Distance
from Redshift

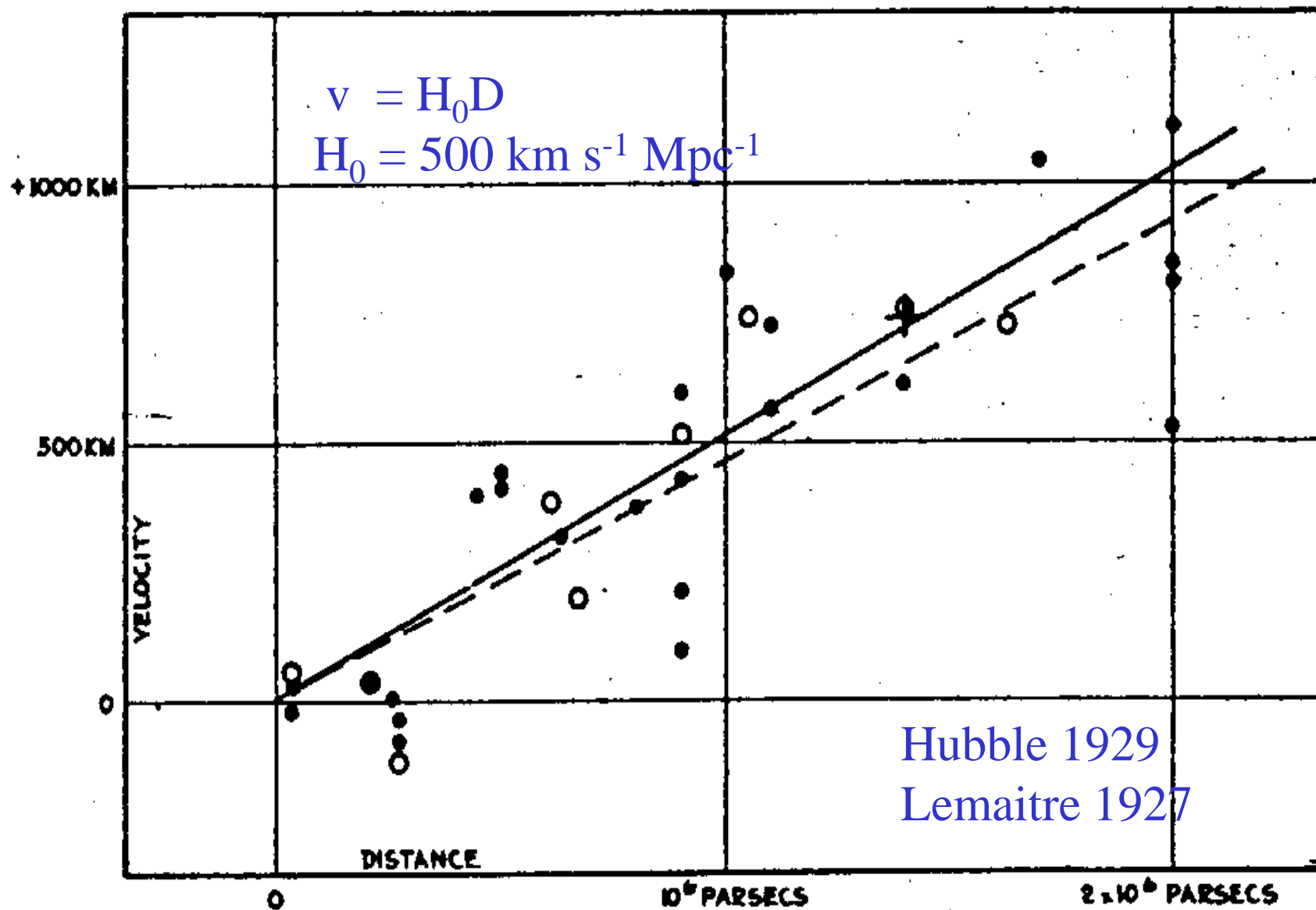


FIGURE 1

$$z=6.4$$



$$1 + z = \frac{S(t_o)}{S(t_e)}$$

The Importance of Hubble's Constant

$$t_0 \sim \frac{1}{H_0}$$

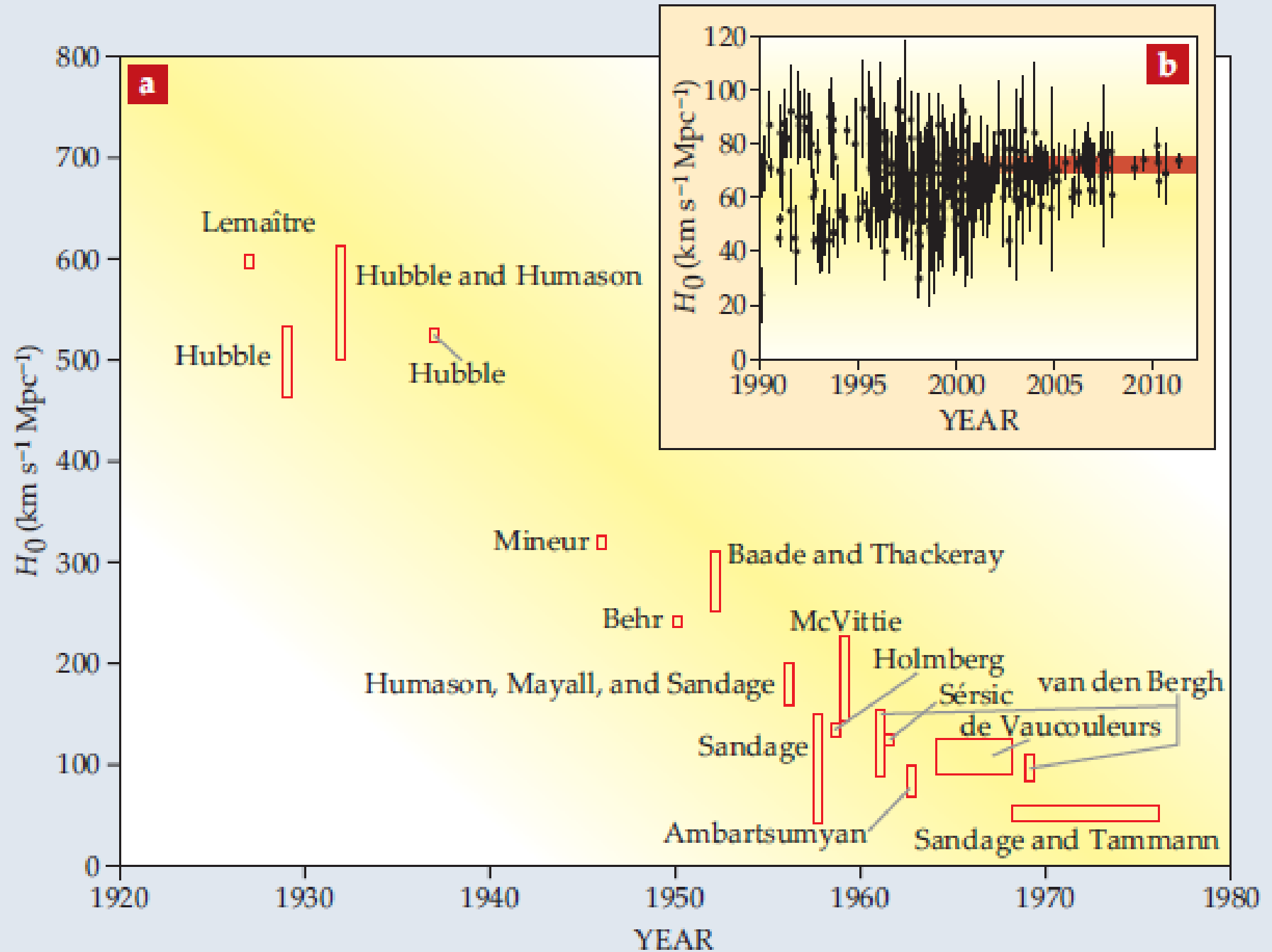
Age of the
Universe

$$R_0 \sim \frac{c}{H_0}$$

Size of the
Universe

$$\rho_c = \frac{3H_0^2}{8\pi G}$$

Critical
Density



Determination of Hubble's Constant



$H_0 = 73 \pm 2$ (random) ± 4 (systematic) km s⁻¹ Mpc⁻¹

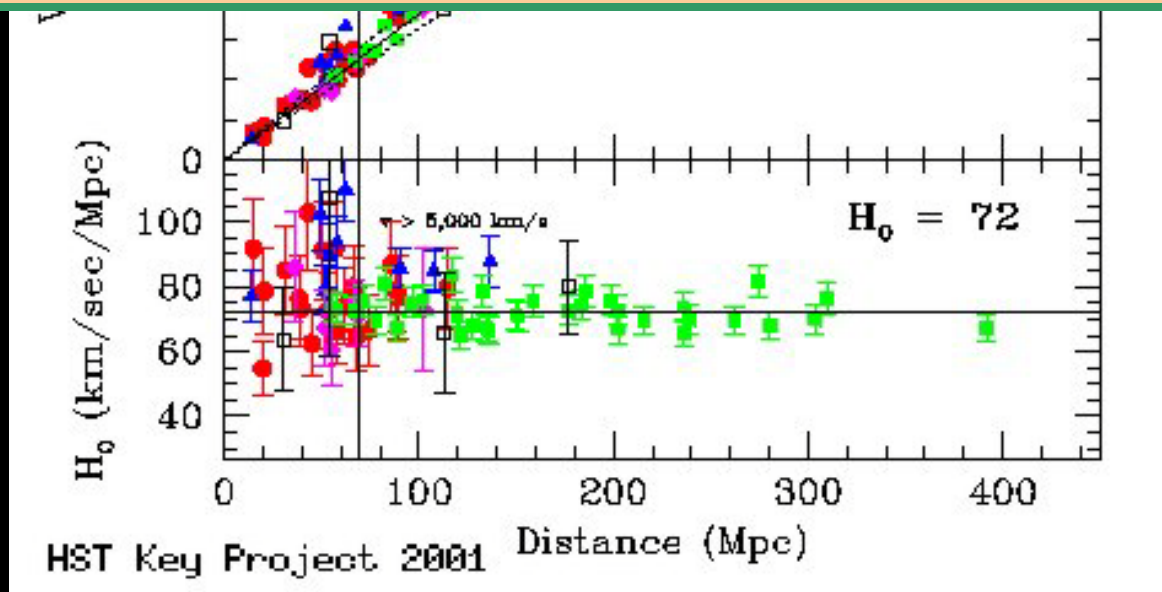


Table 2
Maximum Likelihood Λ CDM Parameters^a

Parameter	Symbol	WMAP Data	Combined Data ^b
Fit Λ CDM Parameters			
Physical baryon density	$\Omega_b h^2$	0.02256	0.02240
Physical cold dark matter density	$\Omega_c h^2$	0.1142	0.1146
Dark energy density ($w = -1$)	Ω_Λ	0.7185	0.7181
Curvature perturbations, $k_0 = 0.002 \text{ Mpc}^{-1}$	$10^9 \Delta_{\mathcal{R}}^2$	2.40	2.43
Scalar spectral index	n_s	0.9710	0.9646
Reionization optical depth	τ	0.0851	0.0800
Derived Parameters			
Age of the universe (Gyr)	t_0	13.76	13.75
Hubble parameter, $H_0 = 100 h \text{ km s}^{-1} \text{ Mpc}^{-1}$	H_0	69.7	69.7
Density fluctuations @ $8 h^{-1} \text{ Mpc}$	σ_8	0.820	0.817
Baryon density/critical density	Ω_b	0.0464	0.0461
Cold dark matter density/critical density	Ω_c	0.235	0.236
Redshift of matter-radiation equality	z_{eq}	3273	3280
Redshift of reionization	z_{reion}	10.36	9.97

Notes.

^a The maximum-likelihood Λ CDM parameters for use in simulations. Mean parameter values, with marginalized uncertainties, are reported in Table 4.

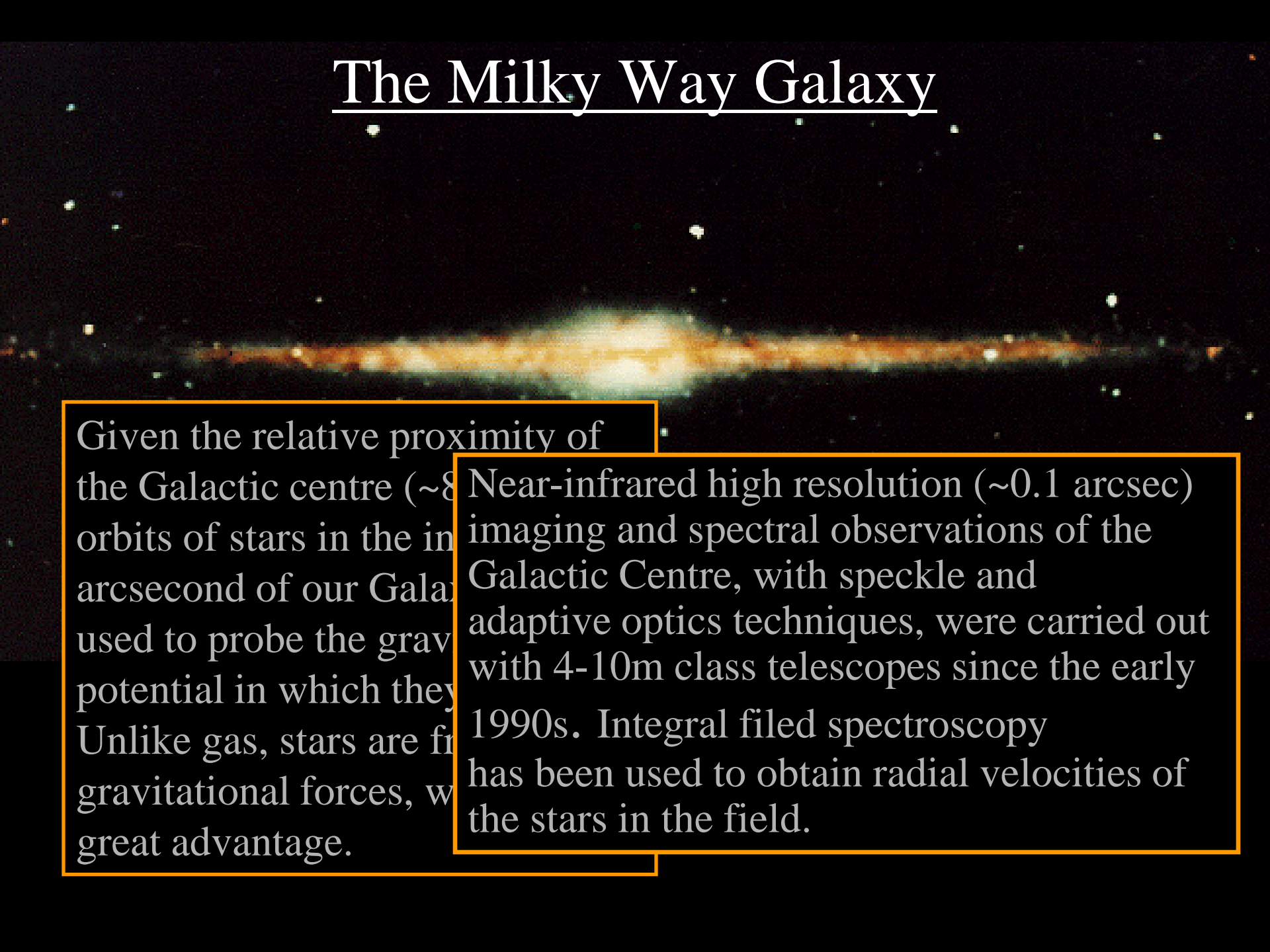
^b “Combined data” refers to WMAP+eCMB+BAO+ H_0 .

WMAP
Hinshaw+ 2013

Super-Massive Black Hole in the Milky Way

Genzel etal,
Ghez etal

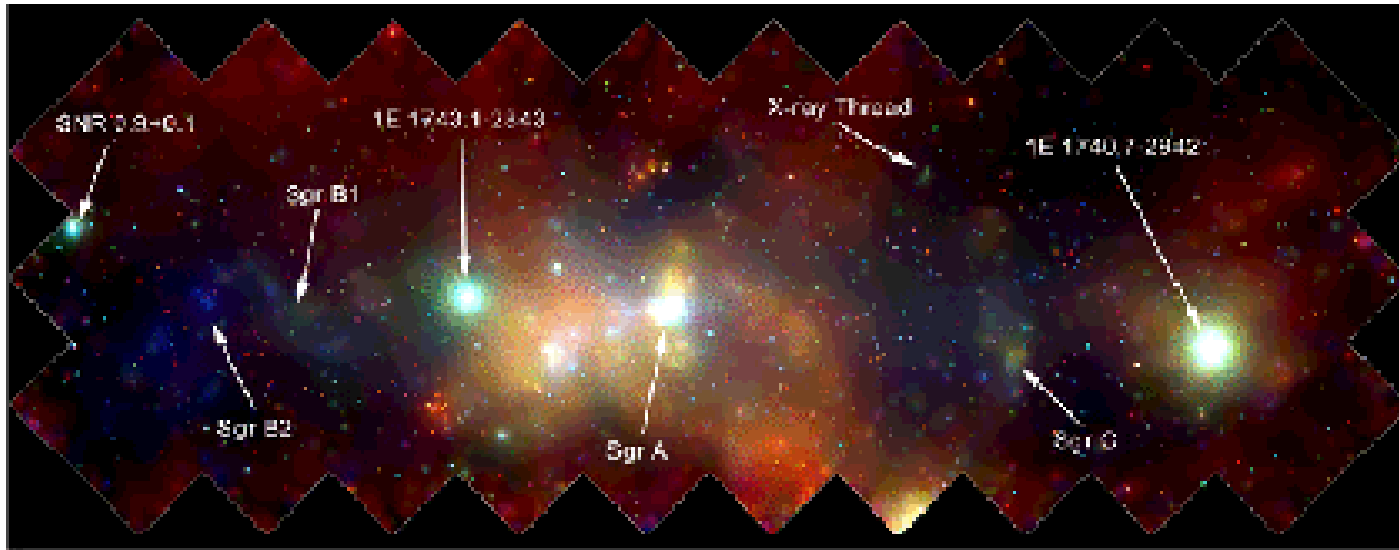
The Milky Way Galaxy



Given the relative proximity of the Galactic centre (~ 8 kpc), imaging and spectral observations of the orbits of stars in the inner Galaxy, within an arcsecond of our Galactic Centre, with speckle and adaptive optics techniques, were carried out used to probe the gravitational potential in which they move. Unlike gas, stars are free from radiative and gravitational forces, with a great advantage.

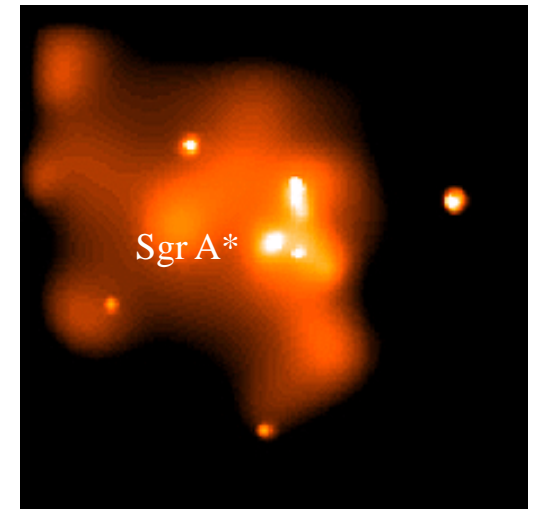
Near-infrared high resolution (~ 0.1 arcsec) imaging and spectral observations of the Galactic Centre, with speckle and adaptive optics techniques, were carried out with 4-10m class telescopes since the early 1990s. Integral field spectroscopy has been used to obtain radial velocities of the stars in the field.

The Galactic Centre



Chandra X-ray mosaic 400x900 light years

Central 10
light years



VLT

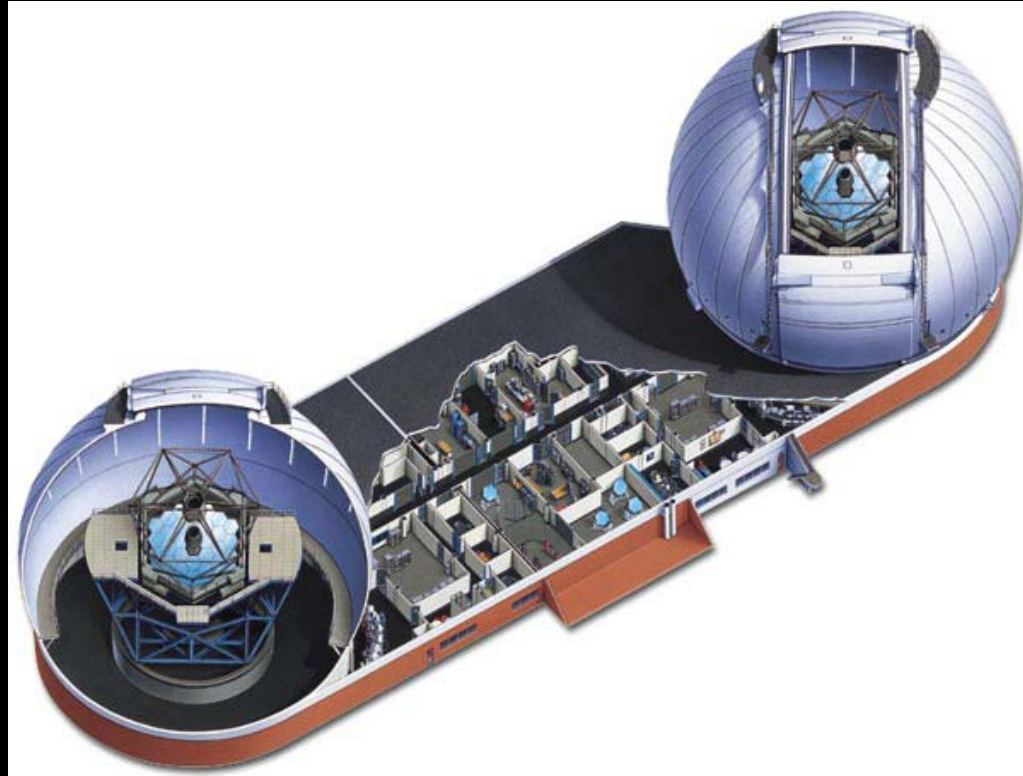
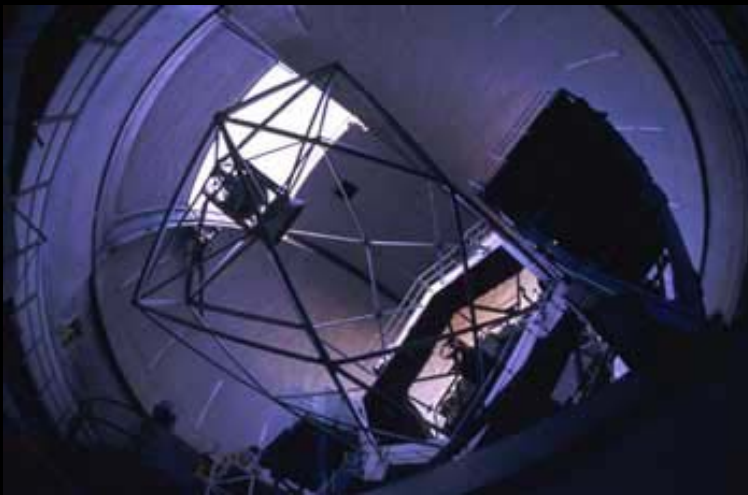


Cerro Paranal, Chile



The Keck Telescopes

Mauna Kea, Hawaii



6 light months

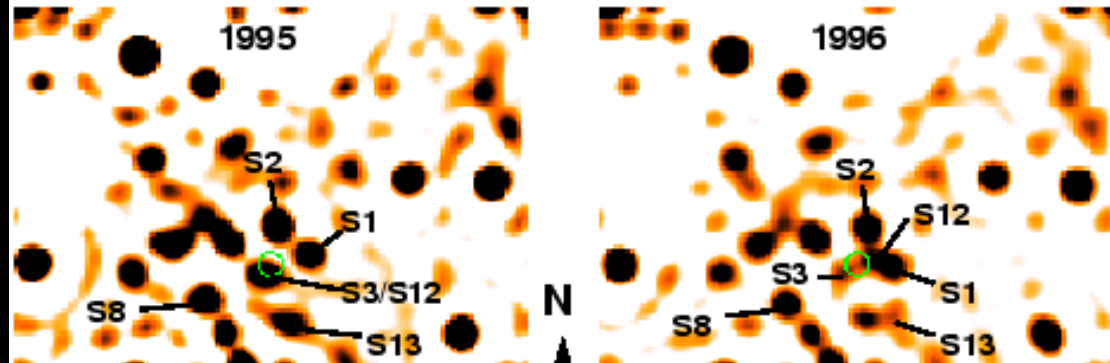


SgrA*

Keck 2 micron

HKL Composite; Speckle
and Adaptive Optics

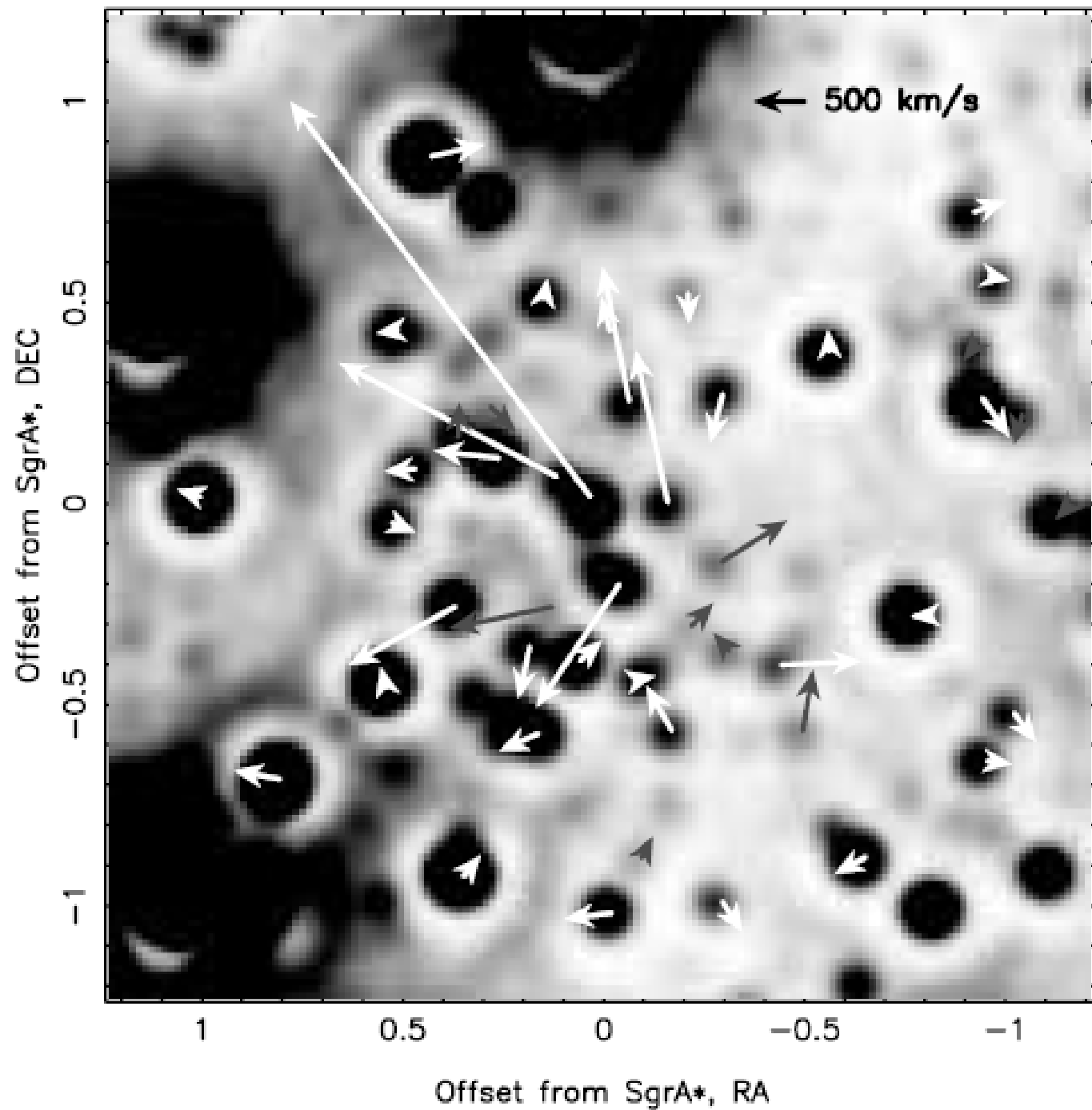
Galactic Centre Stars



Sch The measured positions of stars on the detector have to be
Pr transformed to a common astrometric frame. This is based
mo on eight maser stars for which positions can be determined
wit in radio as well as NIR images. A set of reference stars
hav which are present in both the S-star images as well as the
maser-star images. The reference and maser stars are
themselves in motion, which has to be taken into account.
Positional accuracy upto 1mas, proper motion accuracy of
0.1 mas yr⁻¹ and line-sight-velocity accuracy of 5 km s⁻¹
are obtained.

1"

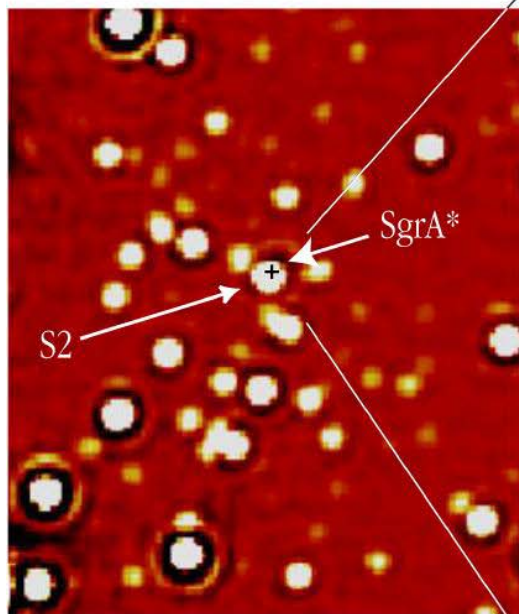
Fig. 3.— Identification of the sources S1, S2, S3, S8, S12, S13, and S14 for the epochs 1995.5, 1996.4, 1999.5, and 2000.5. The circle of ~ 50 mas radius marks the position of Sgr A*.



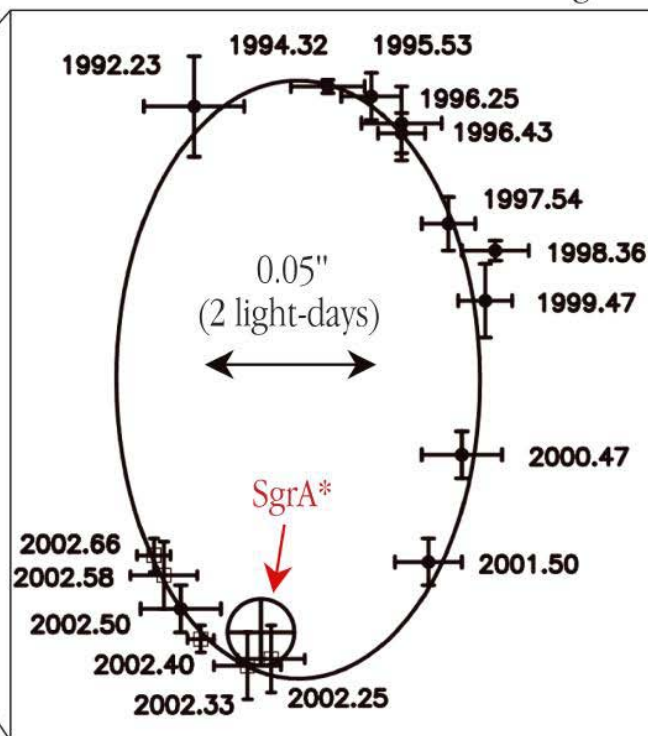
Schodel et al
ApJ 2003

Star Closest to Galactic Centre

NACO May 2002



S2 Orbit around SgrA*



Bound, highly
eccentric (**0.87**) orbit,
period **15.2yr**,
pericentre distance
17 light hours (0.6mpc,
0.015mas),
semi-major axis
4.54mpc
Best fit central point
mass **$3.7 \times 10^6 M_{\text{Sun}}$**

The Motion of a Star around the Central Black Hole in the Milky Way

ESO PR Photo 23c/02 (9 October 2002)

Schodel et.al Nature 2003

© European Southern Observatory



$$0.1 \text{ arcsec} = 3.9 \left(\frac{D}{8 \text{ kpc}} \right) \text{ mpc}$$

ORBITAL PARAMETERS OF S2 AS DETERMINED FOR NORMAL AND EQUAL WEIGHTING
OF THE MEASURED POSITIONS

Parameters (1)	Normal Weighting (2)	Equal Weighting (3)	Ghez et al. ^a (4)
Offset R.A. (mas)	2.0 ± 2.4	1.4 ± 1.3	3.5 ± 2.9
Offset decl. (mas).....	-2.7 ± 4.5	-2.3 ± 3.1	-6.8 ± 4.7
Central mass ($\times 10^6 M_{\odot}$).....	3.31 ± 0.67	3.07 ± 0.72	4.07 ± 0.68
Period (yr).....	15.73 ± 0.74	15.31 ± 0.71	15.78 ± 0.82
Pericenter passage (yr)	2002.31 ± 0.02	2002.31 ± 0.04	2002.33 ± 0.02
Eccentricity	0.87 ± 0.02	0.87 ± 0.02	0.87 ± 0.01
Angle of line of nodes (deg)	45.8 ± 7.0	40.9 ± 8.2	49.9 ± 3.0
Inclination (deg).....	$\pm 45.7 \pm 2.6$	$\pm 44.7 \pm 3.9$	-47.3 ± 2.5
Angle of node to pericenter (deg).....	244.7 ± 4.7	241.0 ± 6.3	248.5 ± 1.8
Semimajor axis (mpc).....	4.54 ± 0.27	4.34 ± 0.31	4.87 ± 0.21
Separation of pericenter (mpc)	0.59 ± 0.10	0.56 ± 0.10	0.62 ± 0.03

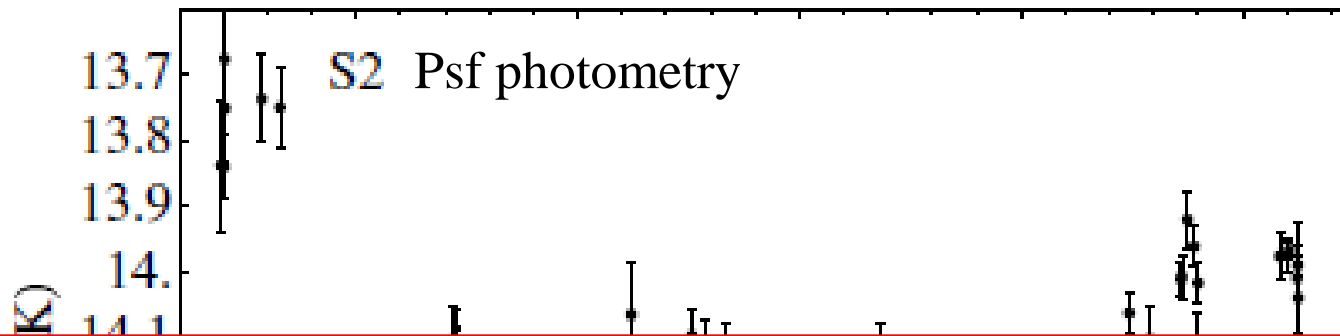
$$M = 3.31 \times 10^6 M_{\odot}, \quad P = 15.7 \text{ yr}, \quad D_{\text{peri}} = 0.59 \text{ mpc}$$

Schodel et al ApJ 2003

Photometry Around Peristron Passage of S2

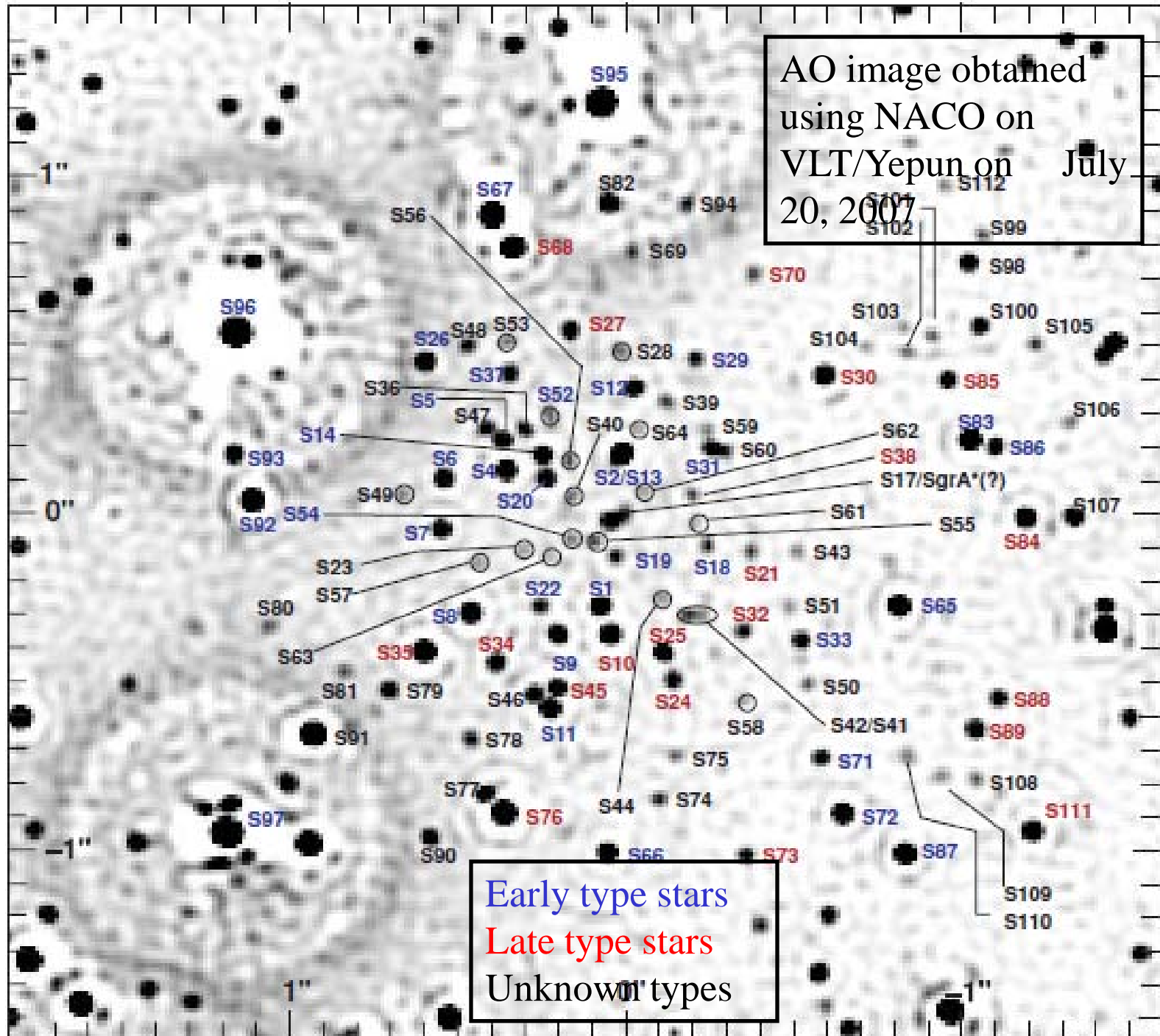
S2 is one of the brightest in the sample and has been

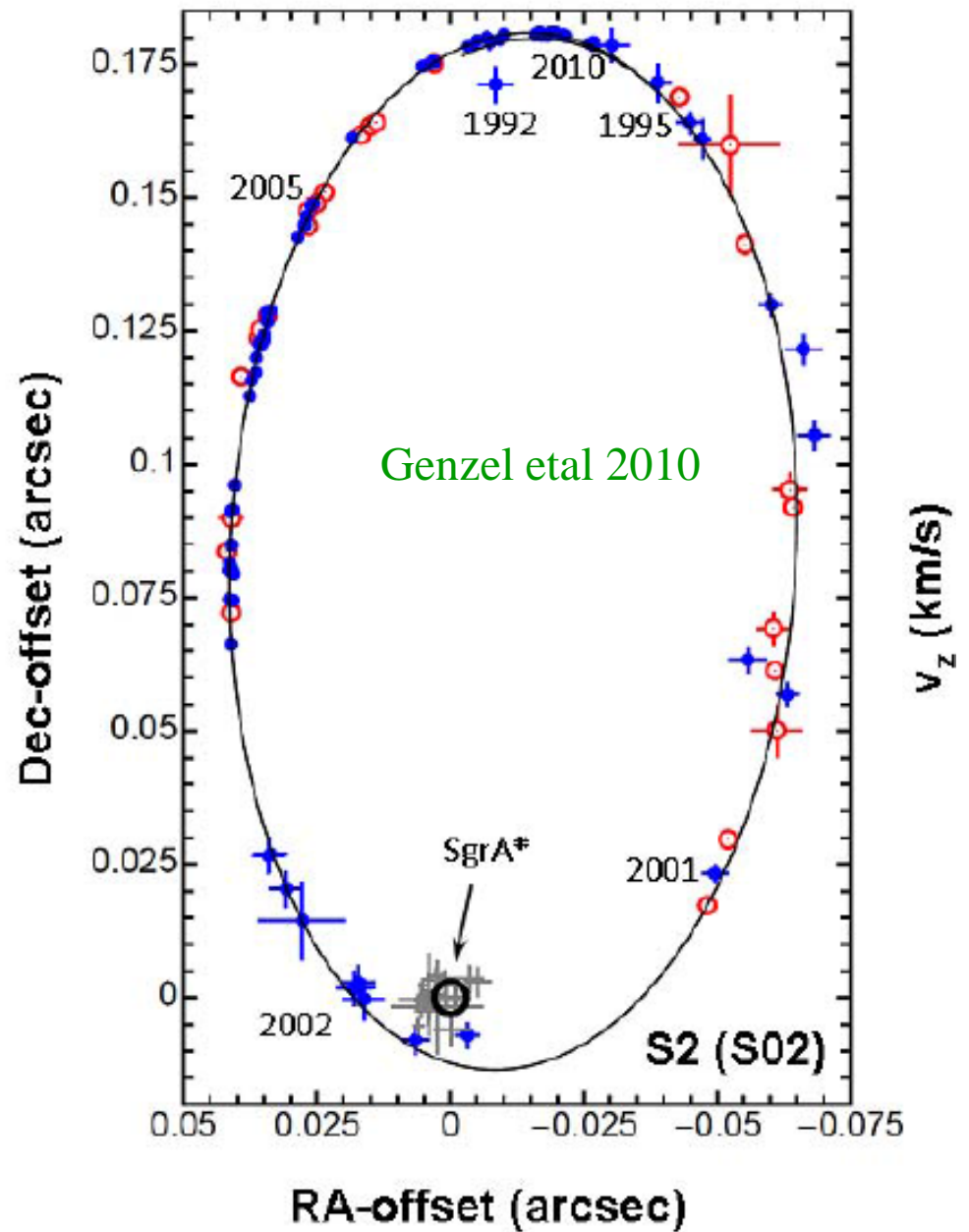
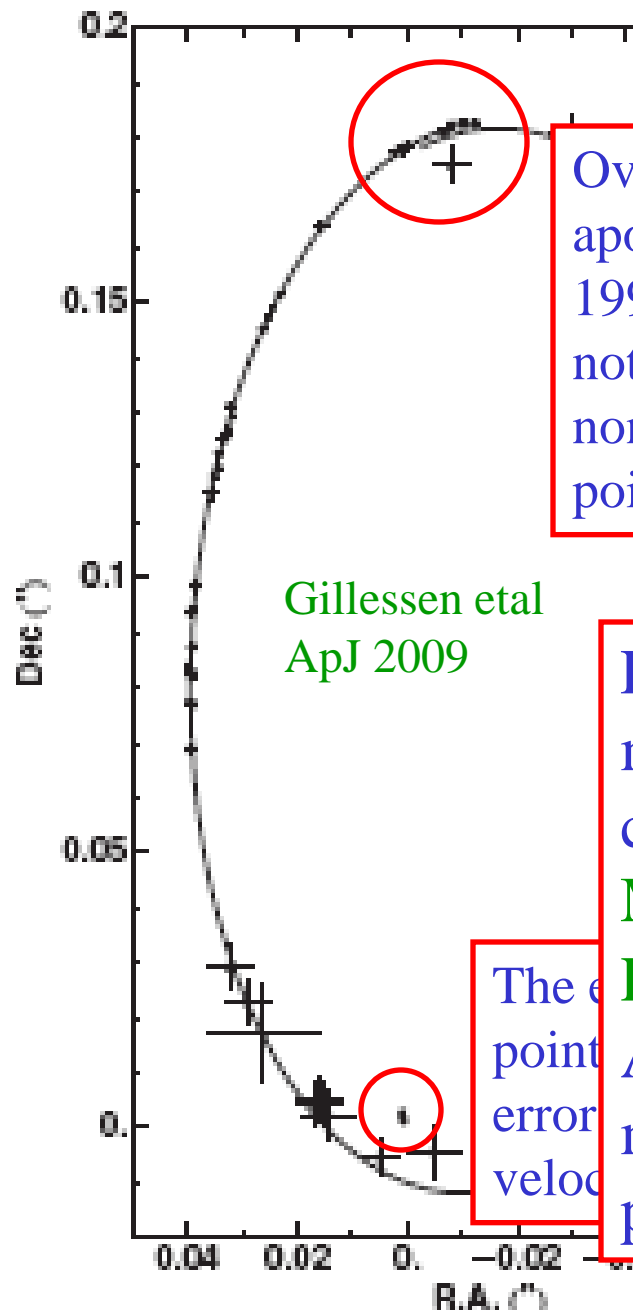
observed
periodic
partially
the bright
peris



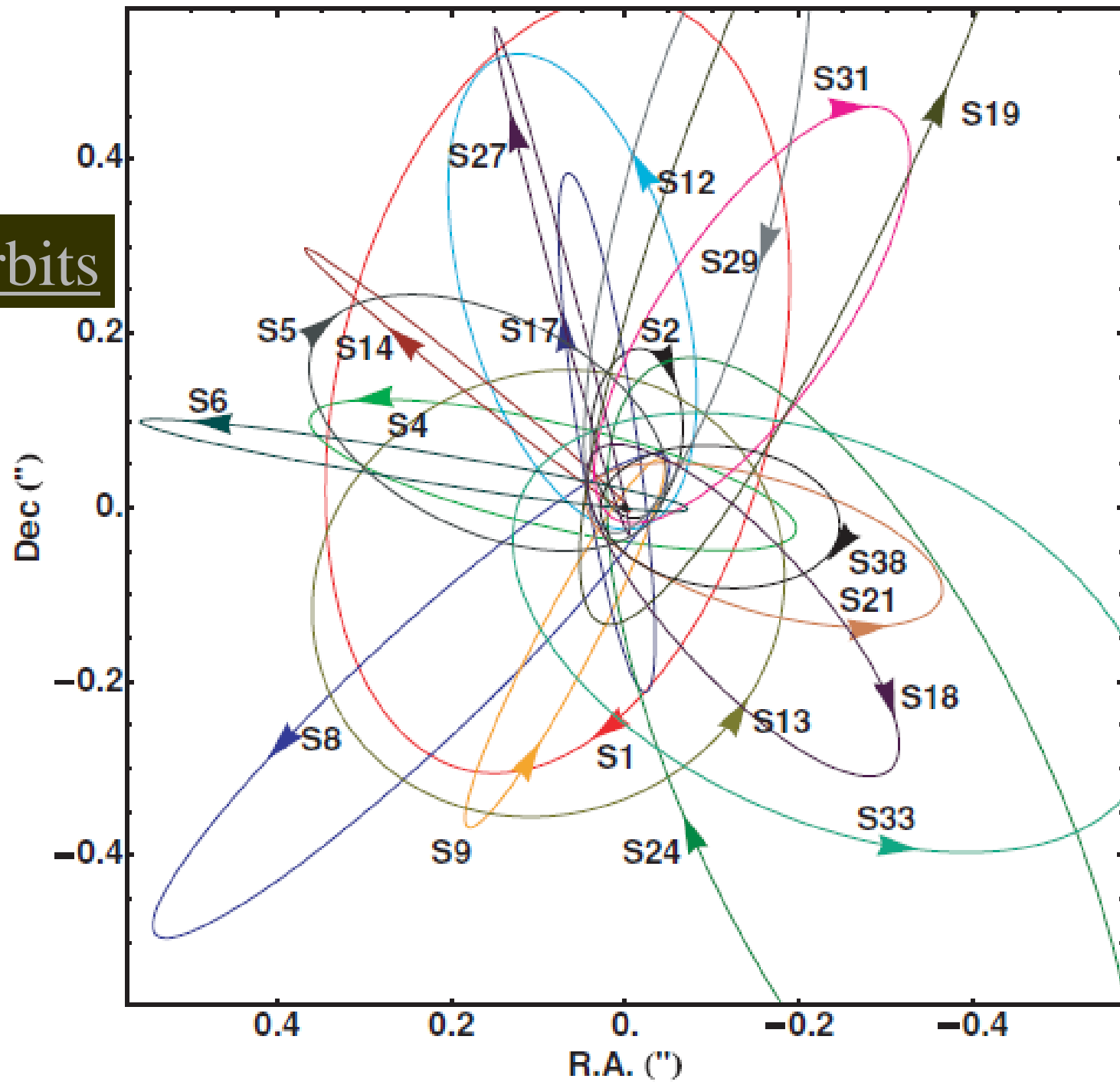
Viable explanations for the change in brightness of S2 are (1) Reduced extinction due to removal of dust by Sgr A* which should effect other stars as well as can be tested in the future; (2) Dust in the accretion flow onto the black hole could be heated by S2 and produce the excess brightness; (3) S2 could be confused with another star. The last two possibilities would lead to astrometric errors, affecting the computed orbit.

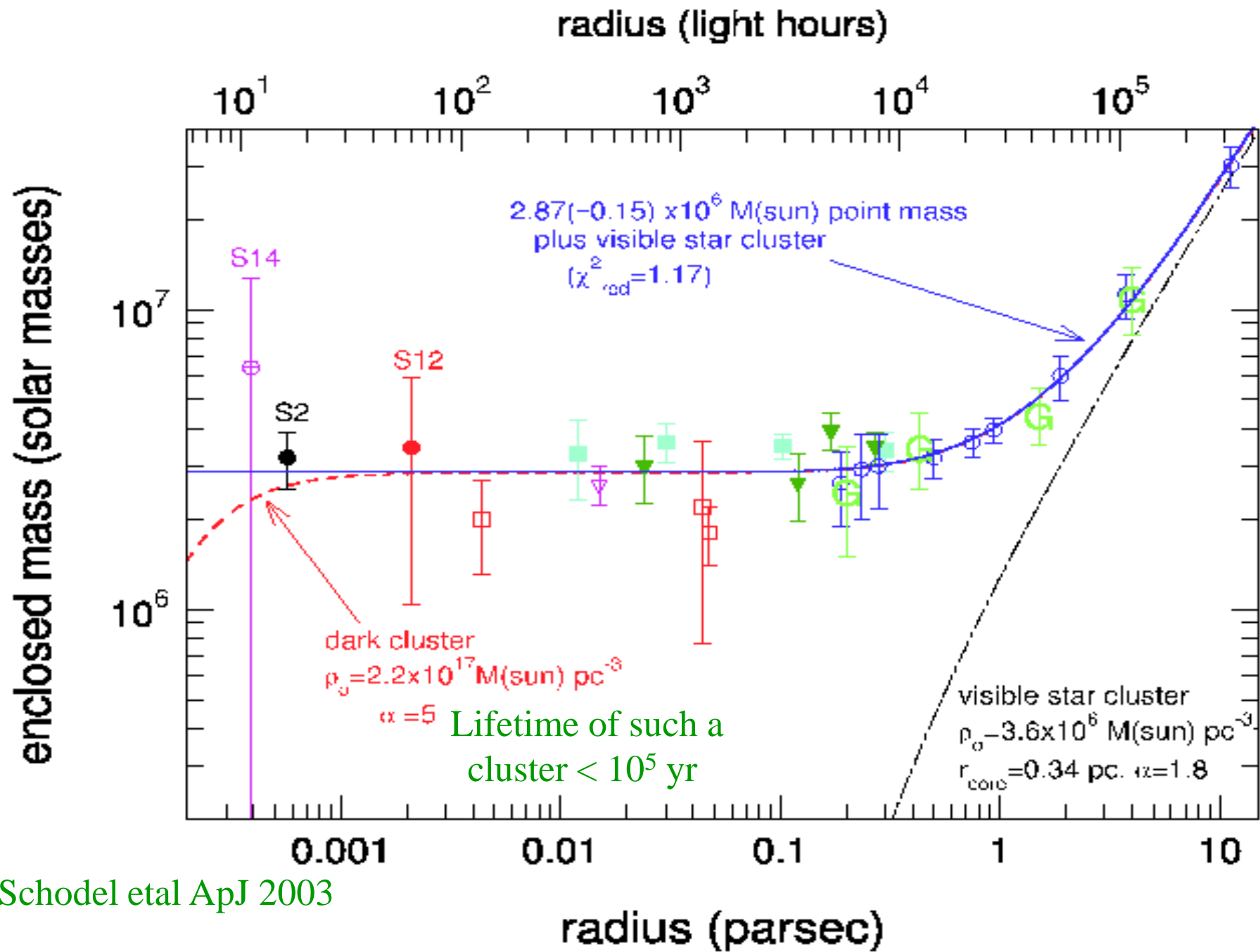
AO image obtained
using NACO on
VLT/Yepun on July
20, 2007



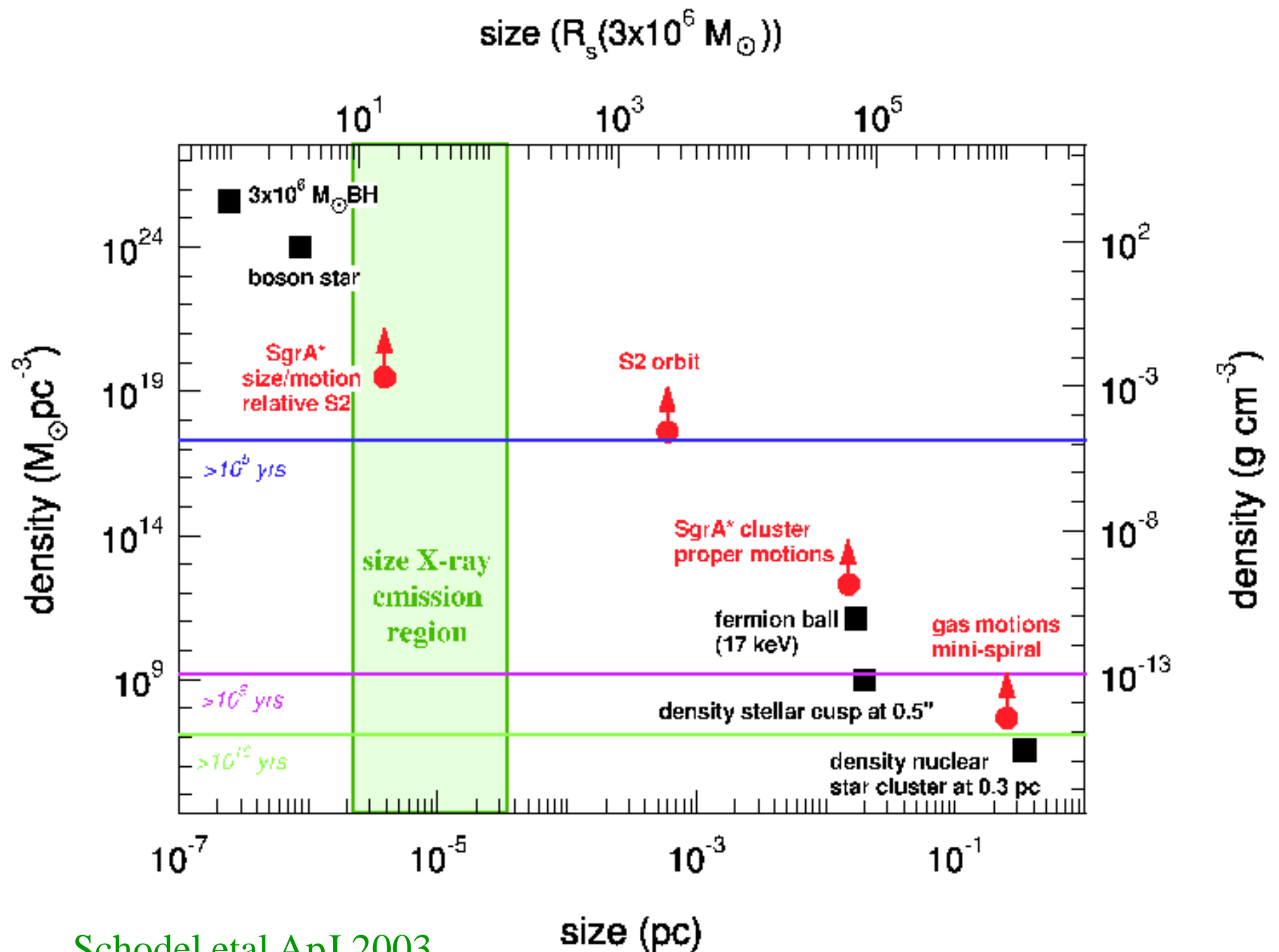


Stellar Orbits





Schodel et al ApJ 2003

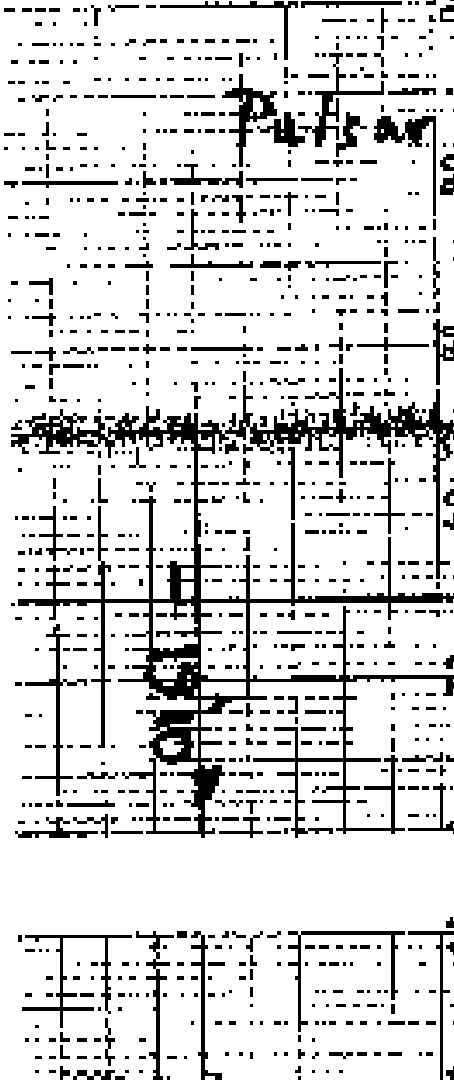


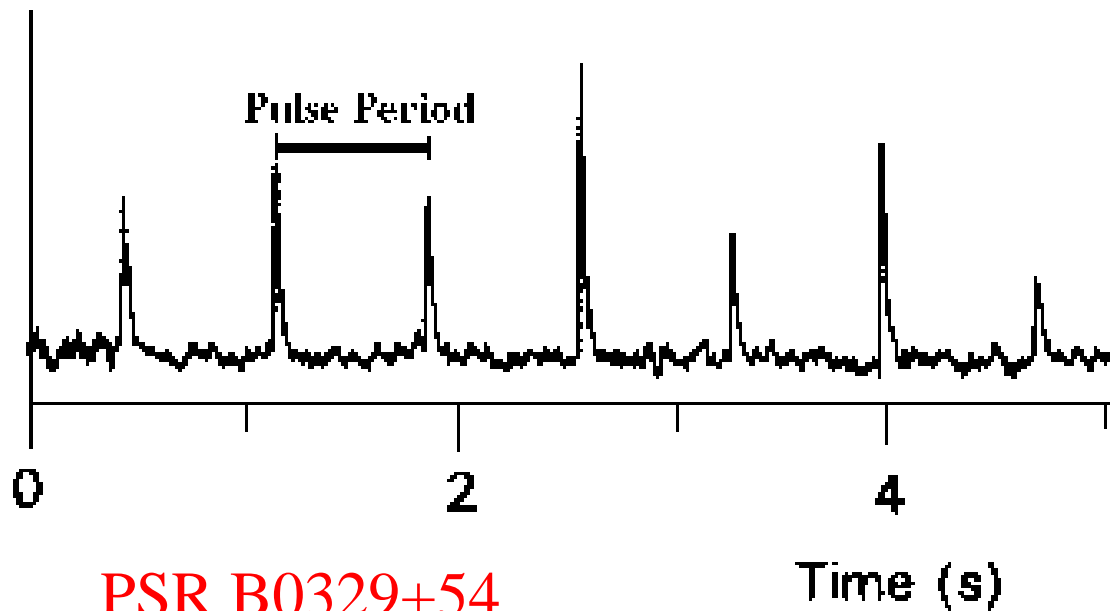
Schodel et al ApJ 2003

Pulsars as Cosmic Clocks

Discovery of Radio Pulsars

(a)





PSR B0329+54

Distance 2643 light years

$P = 0.71452 \text{ s}$

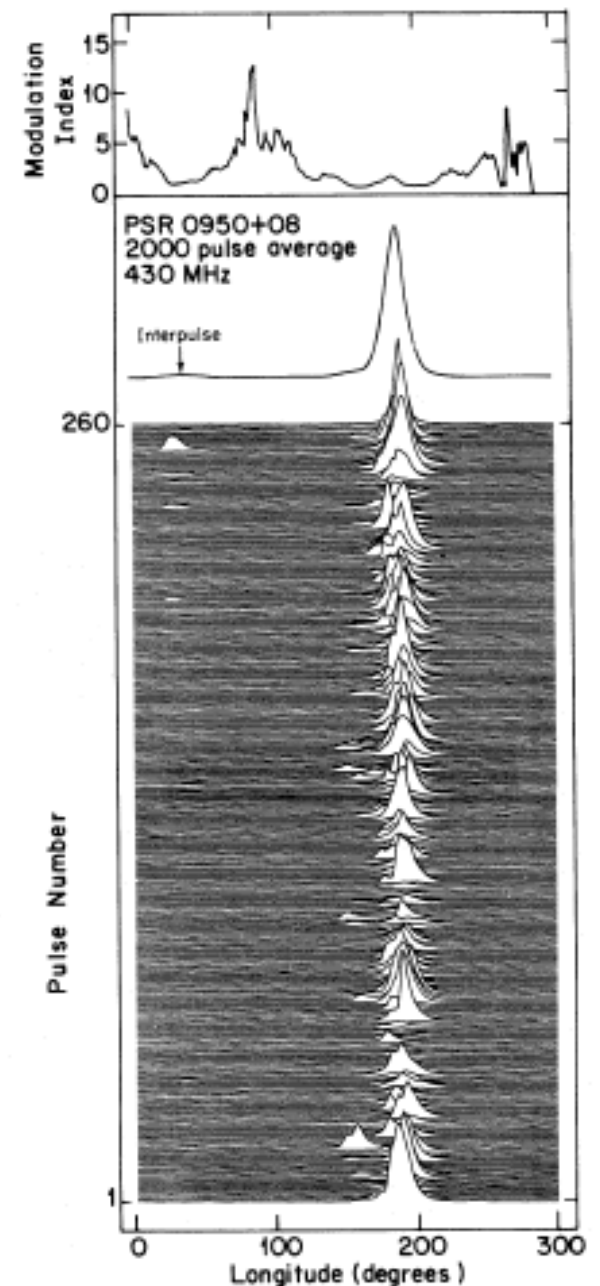
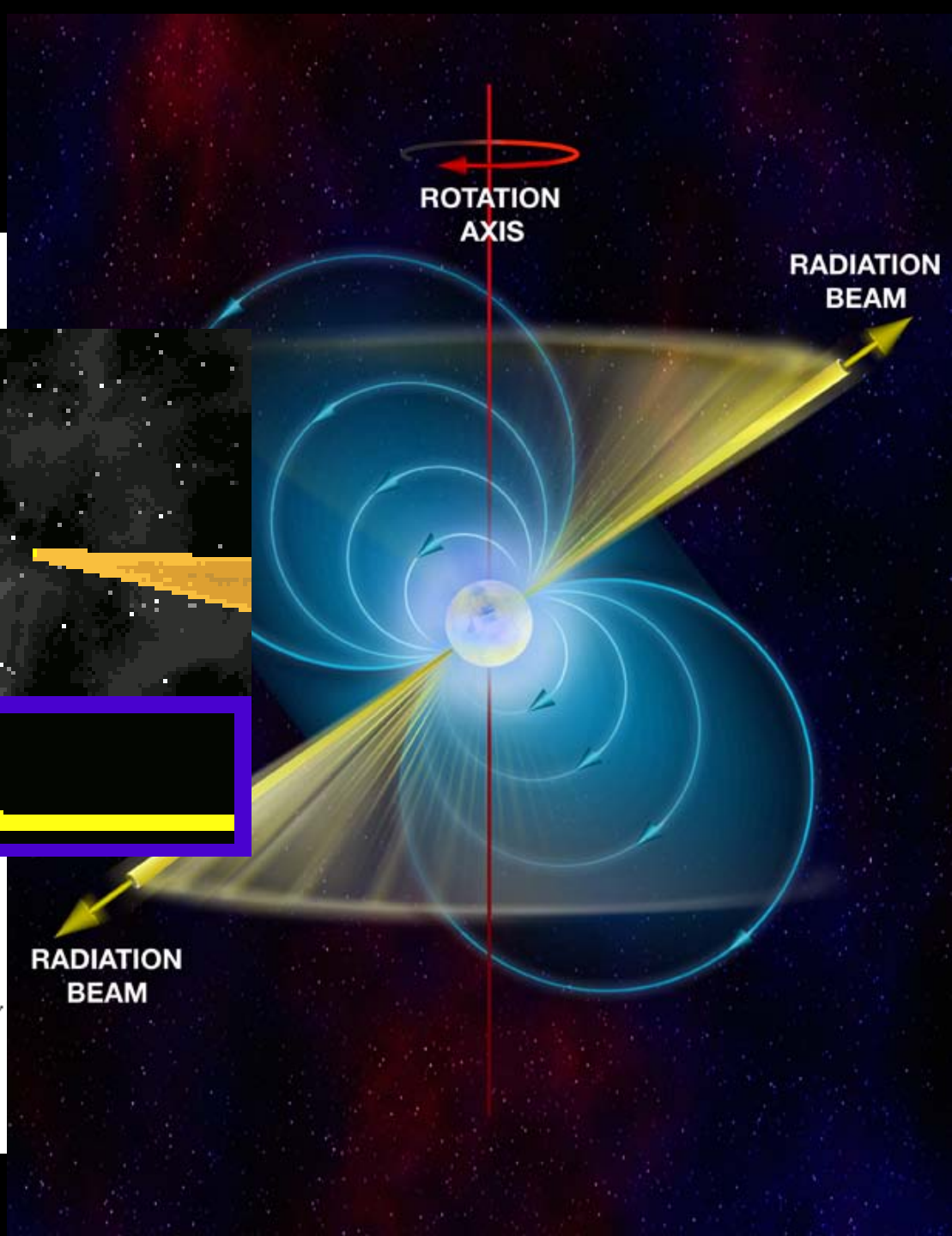
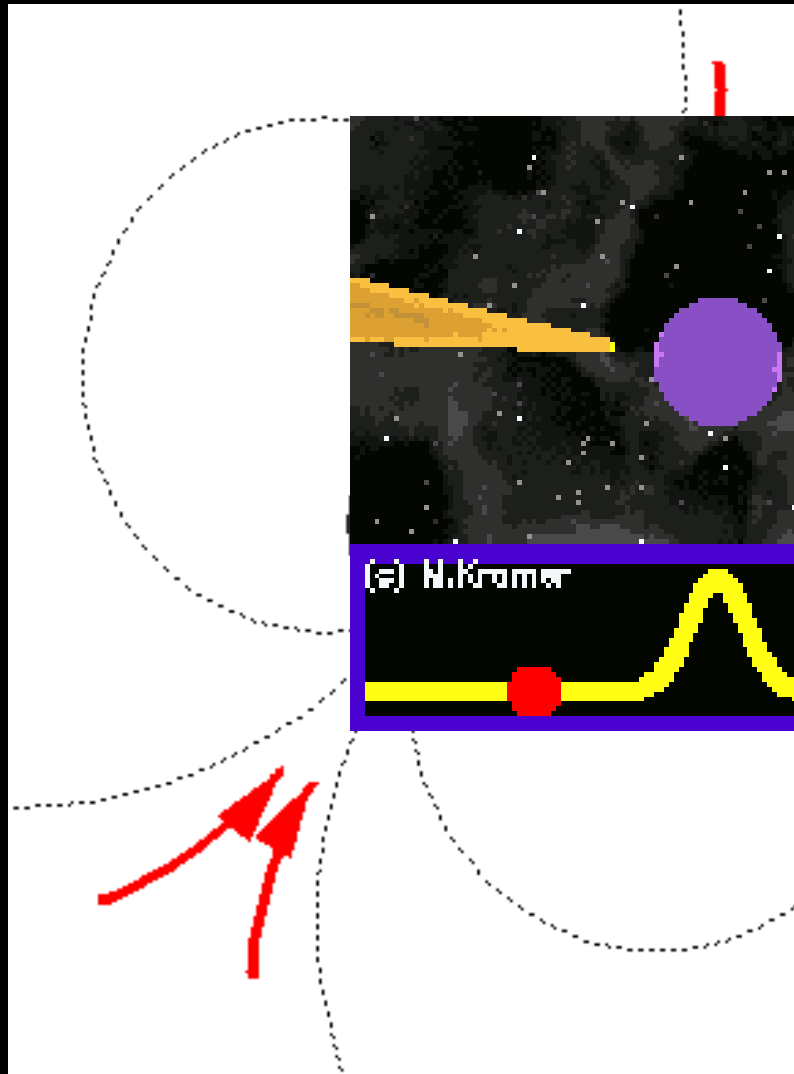


FIG. 5.—A sequence of 260 pulses that shows strong subpulses at the position of the interpulse. Also plotted is the modulation index [eq. (1)].

Pulsars as Neutron Stars



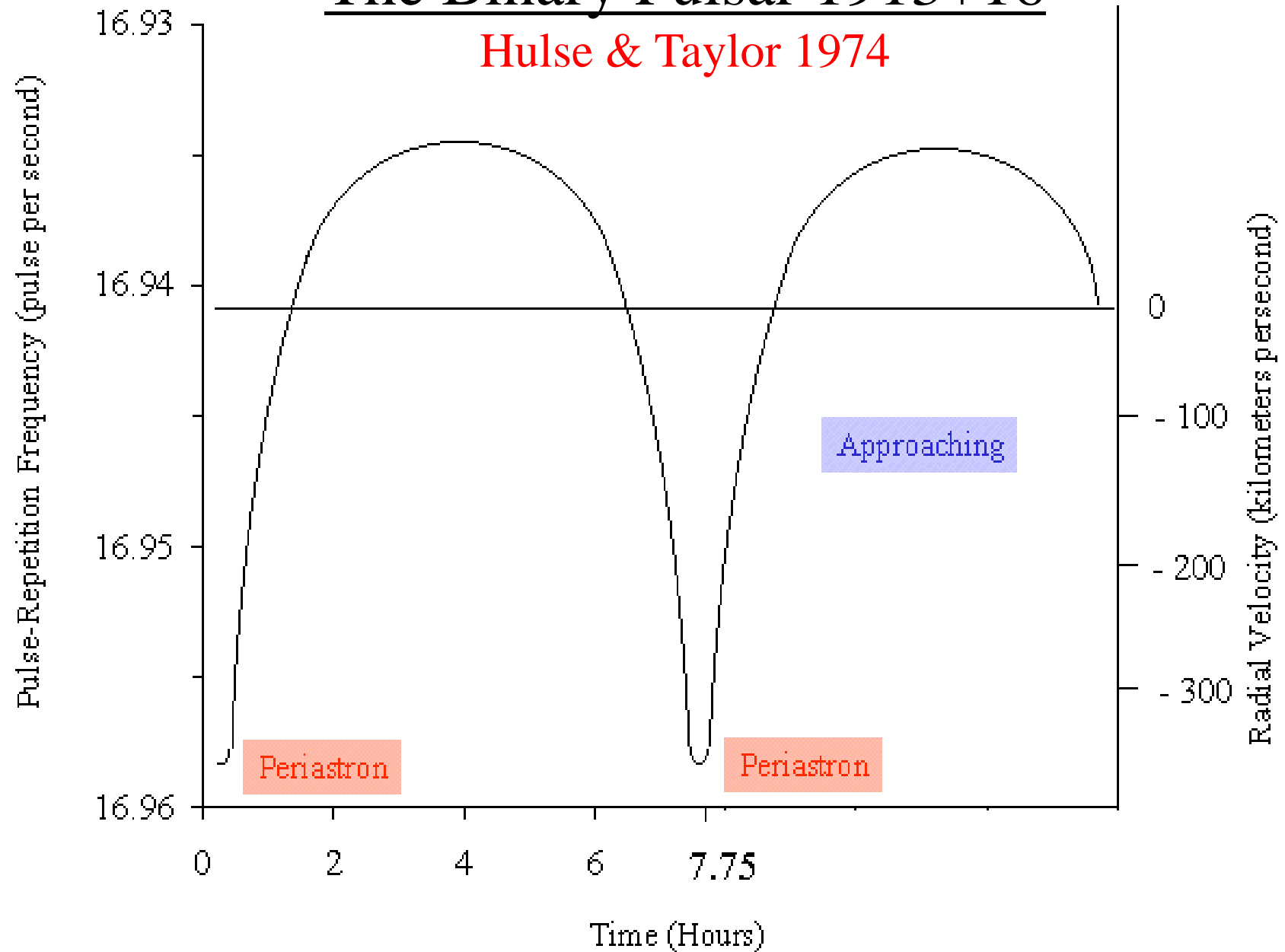
Pulsar Periods and Period Derivatives

Determination of accurate pulsar periods requires many corrections to observations:

- Pulse dispersion due to the interstellar medium
- Earth's motion in an elliptic orbit
- Motion of the Sun relative to the barycentre
- Relativistic corrections
- Orbital motion of the pulsar around a companion
- Slowing down of pulsar's rotation...

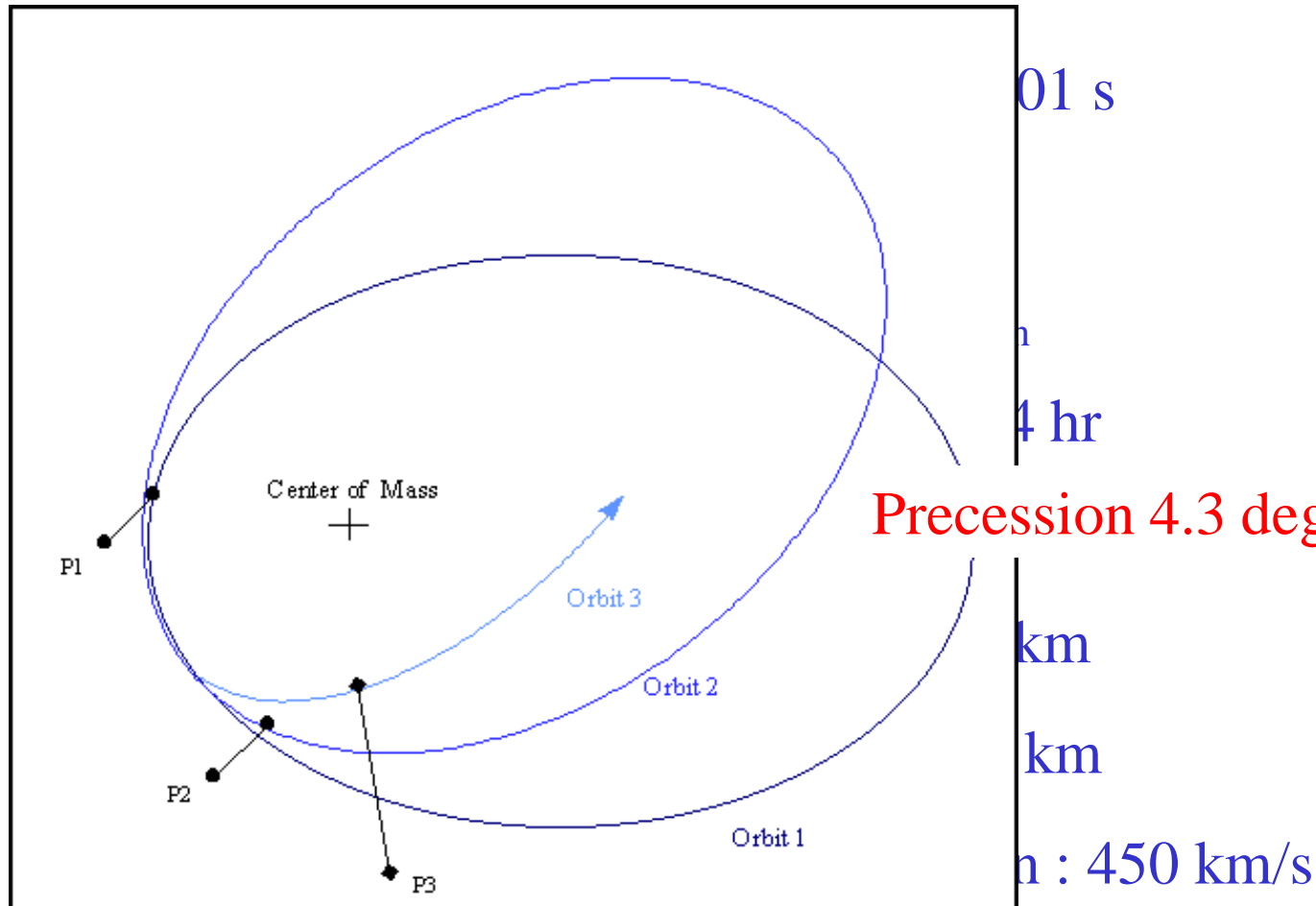
The Binary Pulsar 1913+16

Hulse & Taylor 1974



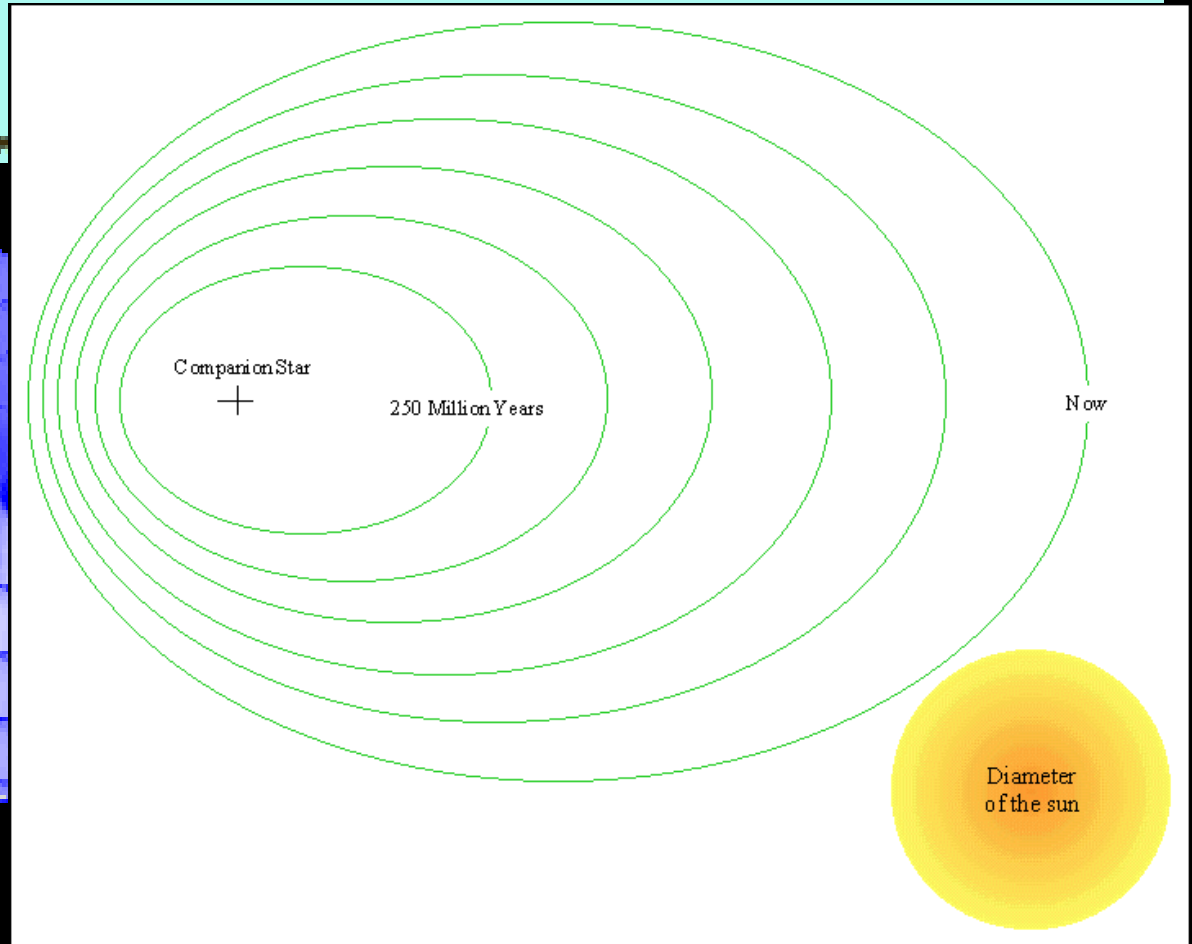
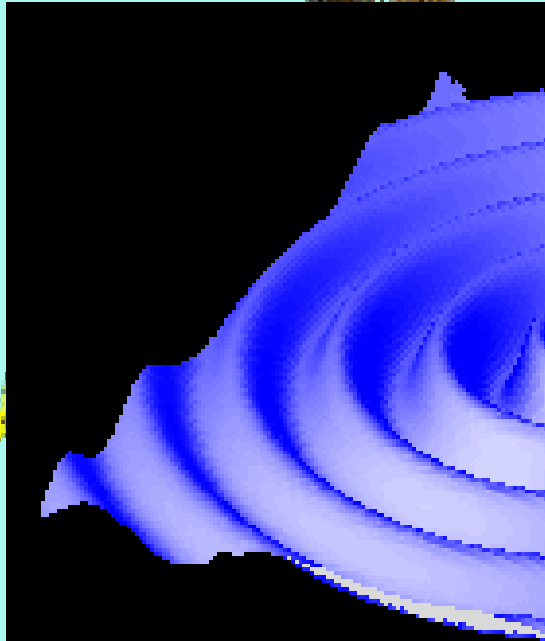
The Binary Pulsar 1913+16

Hulse & Taylor 1974



CM Orbital velocity of stars at apastron: 110 km/s

radio signals
to Earth



The Binary Pulsar

1913+16

Hulse & Taylor 1974

The Binary Pulsar

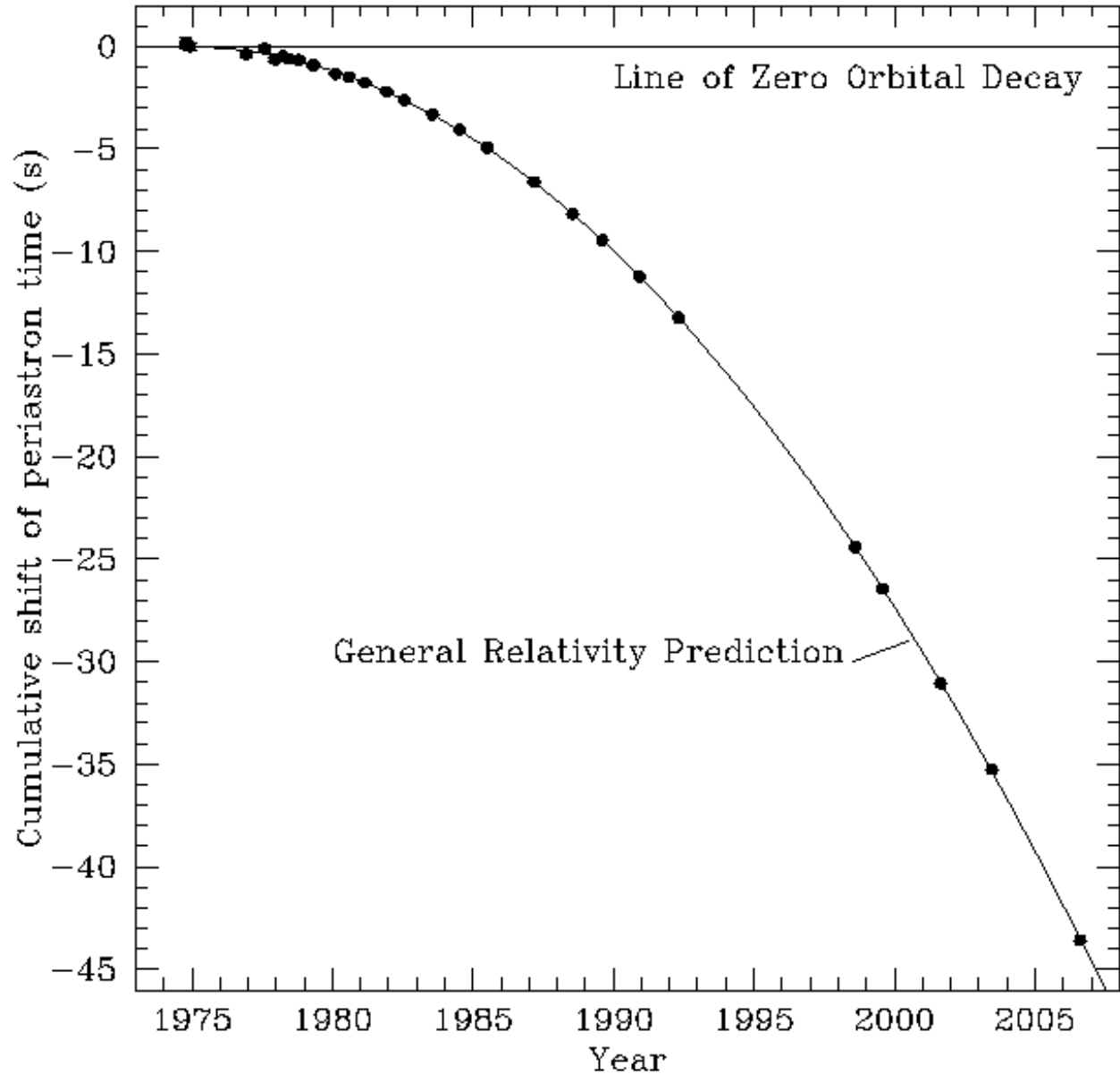
1913+16

Hulse & Taylor 1974

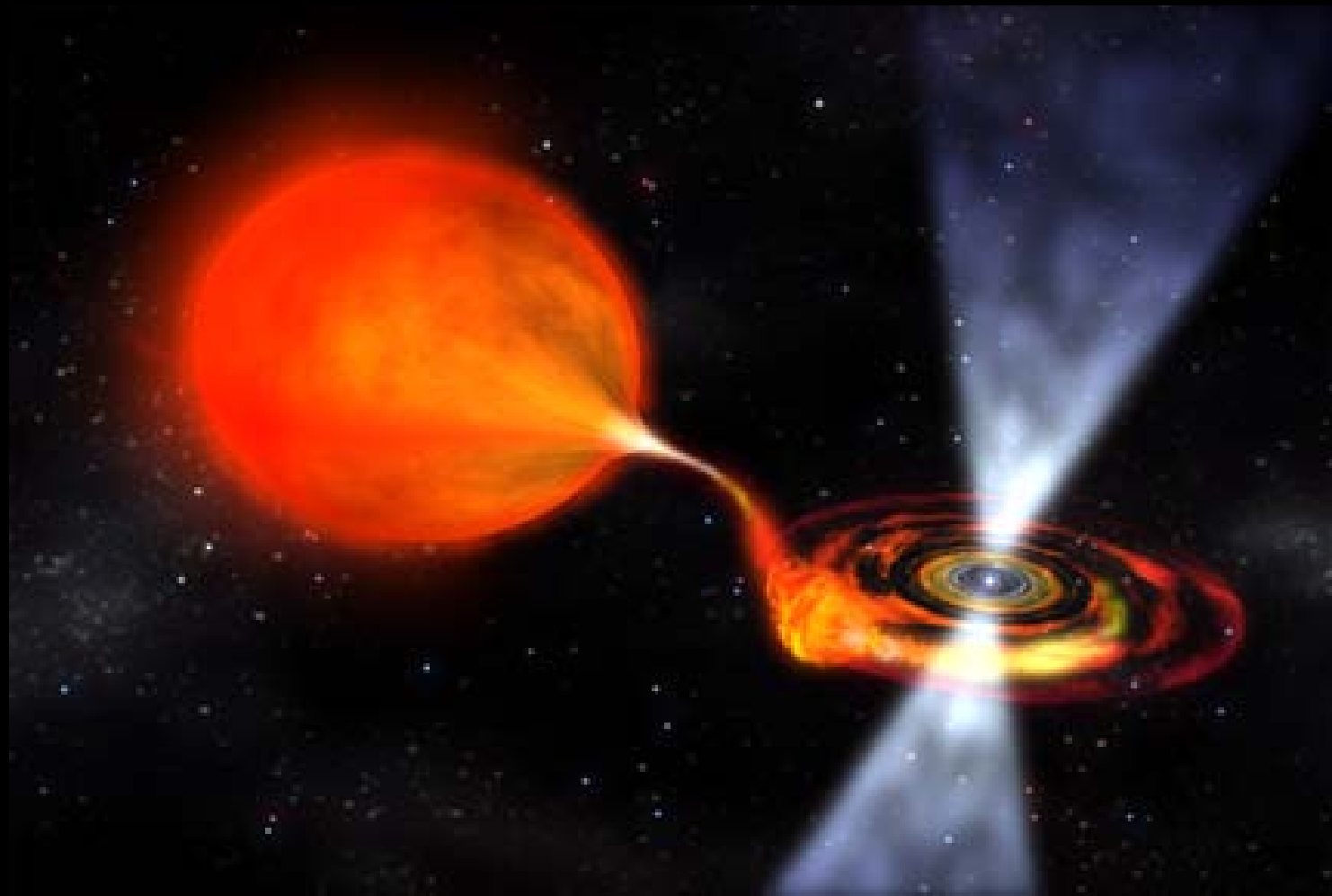
Orbital decay due to
the emission of
gravitational waves

$$\frac{dP}{dt} = -3.4 \times 10^{-12} \left(\frac{M}{M_{\odot}} \right)^{5/3} \left(\frac{P}{1h} \right)^{-5/3}$$

$$M = 1.4M_{\odot}, P = 7.75h$$



Millisecond Pulsars

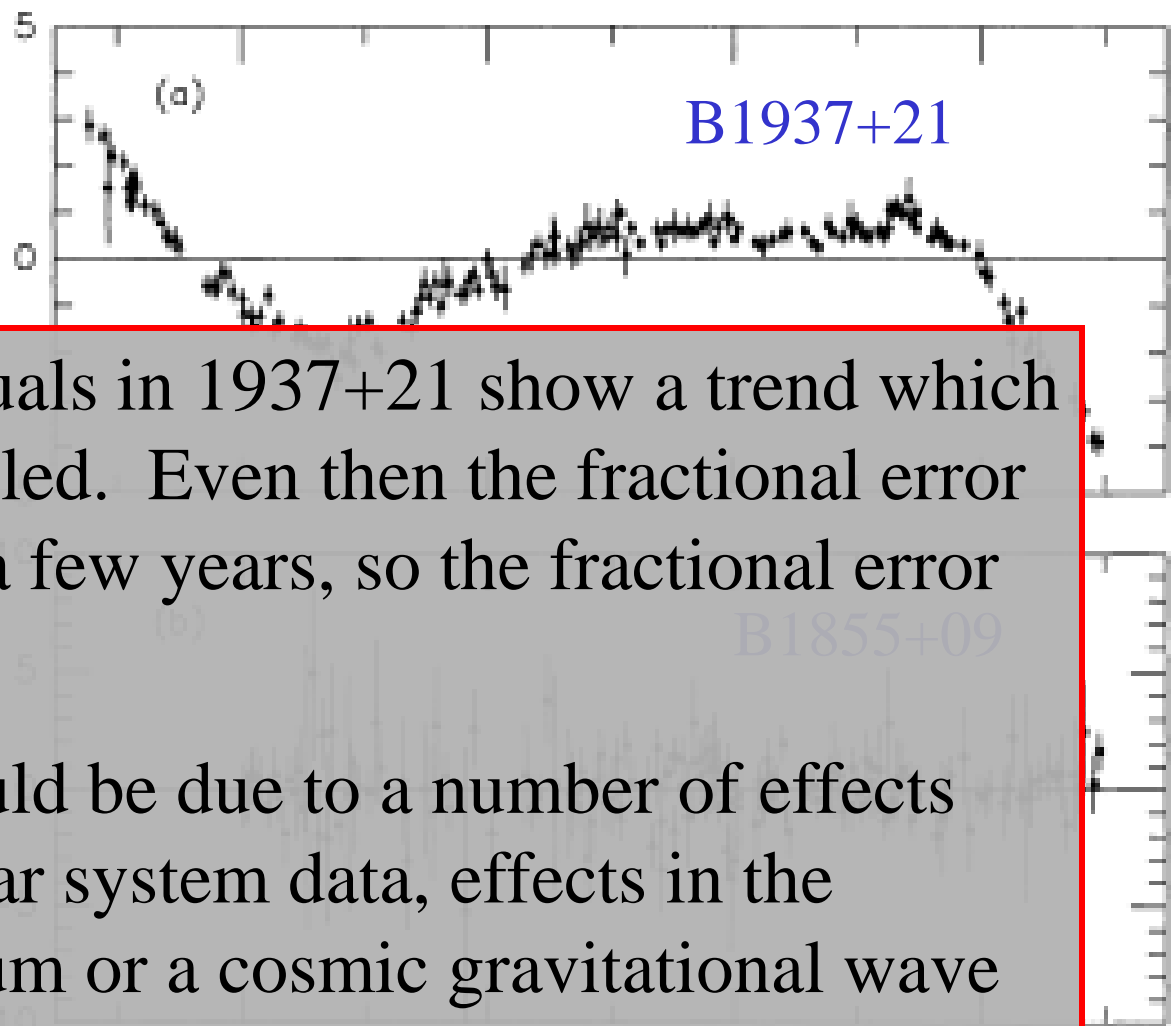


Millisecond Pulsar

Periods and Period Derivatives

J1748-24	1. 395, 954, 82 ms 6	0 x 10 ⁻¹⁹ s s ⁻¹
B1937+21	1. 557, 806, 472, 448, 817 ms 3	1.051212 x 10 ⁻¹⁹
B1957+20	1. 607, 401, 684, 806, 32 ms 3	1.68515 x 10 ⁻²⁰

Timing Residuals



The timing residuals in 1937+21 show a trend which remains unmodelled. Even then the fractional error is a few μs over a few years, so the fractional error is $\sim 2 \times 10^{-14}$.

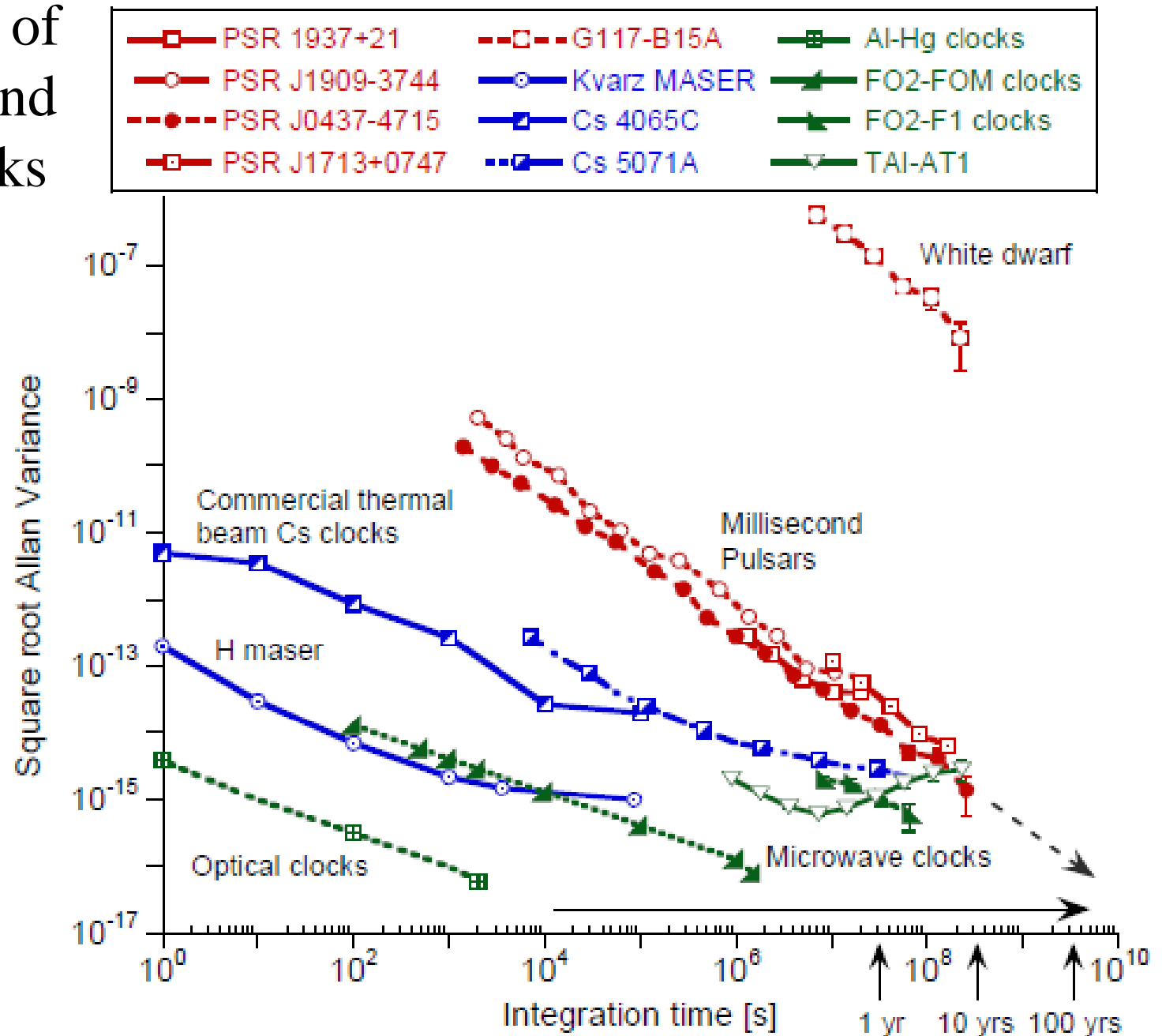
The residuals could be due to a number of effects like incorrect solar system data, effects in the interstellar medium or a cosmic gravitational wave background or even due to clock instabilities.

FIG. 5.—Timing residuals for (a) PSR B1937 + 21 and (b) PSR B1855 + 09, relative to the parameters listed in Table 2 (with $\bar{v} = \dot{\omega} = \dot{x} = \dot{e} = \dot{P}_b = 0$). For clarity we have included only the highest quality data: for PSR B1937 + 21, the DM-corrected TOAs obtained at 2380 MHz with observing systems B (*triangles*) and F (*filled circles*), and for PSR B1855 + 09, those obtained at 1408 MHz with observing systems A (*triangles*) and D (*filled circles*).

Millisecond Pulsars as Accurate Clocks

- For millisecond pulsars, pulse arrival times can be very accurately predicted over many years.
- Such a pulsar can therefore serve as an accurate clock, providing a new timescale which is astronomical in nature.
- Can such time scale compare in precision with the best atomic and optical clocks?
- It is possible that over a long period of time, an array of millisecond pulsars can do better than the best terrestrial clocks now available.

Comparison of Terrestrial and Pulsar Clocks



SKA



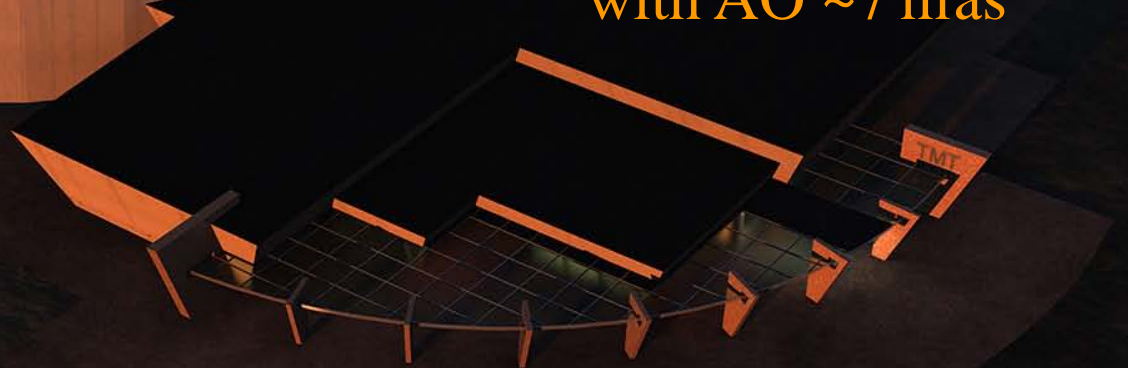
South Africa – Australia
2020, 2024
~3000 dishes, 15m diameter
70MHz-10GHz, $<0.1''$

45 TB/sec
existing correlators
500 PB/yr
archival data
Hexaflop computing

Thirty Meter Telescope

30m equivalent
primary mirror,
492 segments,
1.4m each.
FOV 20 arcmin,
0.31 to 28 micron,
Angular resolution
with AO ~ 7 mas

Caltech
University of California
Canada
Japan
China
India





Thank You!